ESCUELA SUPERIOR POLITÉCNICA DEL LITORAL

Facultad de Ingeniería Marítima y Ciencias del Mar

“Wind Sensitivity and Coastal Ocean Response Analysis of the Mississippi Sound - A Modeling Study”

CAPSTONE PROJECT REPORT

Prior to receiving the degree of:

Oceanographic Engineer

Presented by:

Karen Elizabeth Aguirre Rojas

GUAYAQUIL - ECUADOR

YEAR: 2021

DEDICATION

I dedicate this project to me, for my perseverance, patience, courage, and vision of the world.

To my husband, family and friends for their constant support and motivation during my undergraduate studies.

Thank you. We did it!

ACKNOWLEDGEMENTS

My sincere thanks to ESPOL for having forged a great professional in me. Thanks to Brandy, Jerry, Kemal, and USM for opening the doors of their institution to me, for guiding and teaching me with patience and enthusiasm.

My greatest gratitude and respect to my tutor Iván Saltos and each of my teachers for their admirable vocation and for being a source of knowledge and inspiration.

Last but not least, I thank the person who walked with me since my first semester, who has given me his friendship, support, and wisdom at every stage of my life. Thank you, Herman, for always being there.

EXPRESS STATEMENT

“The responsibility and authorship of the content of this Graduation Project, corresponds exclusively to me; *Karen Elizabeth Aguirre Rojas* and I give my consent to ESPOL to publicly communicate the project by any means to promote consultation, diffusion and public use of intellectual production”

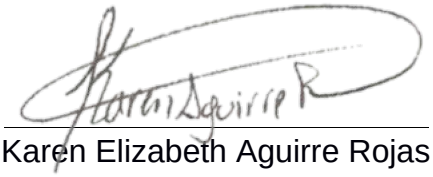

Karen Elizabeth Aguirre Rojas

EVALUATION COURT

Firmado electrónicamente por:
LUIS MIGUEL ALTAMIRANO PEREZ

Luis Altamirano M.Sc.

EVALUATOR

IVAN MARCELO SALTOS ANDRADE

Firmado digitalmente por IVAN MARCELO SALTOS ANDRADE
Fecha: 2021.10.18 14:45:13 -05'00'

Iván Saltos M.Sc.

ADVISOR

RESUMEN

Mississippi Sound es un sistema estuarino de aguas poco profundas separado de las aguas del Golfo de México por islas barrera; caracterizado por sus fuertes frentes climáticos, tormentas y huracanes que afectan los factores hidrodinámicos y morfológicos del área. En este estudio, se utiliza un sistema de modelado numérico para estudiar los efectos del viento en entornos costeros, ensenadas e intercambios de agua. Se desarrolló un algoritmo computacional en MATLAB que filtra e interpola el archivo de fuerza de viento obtenido a través del producto High-Resolution Rapid Refresh (HRRR) para modelar ambos sets de datos (sin filtrar y filtrados) en el modelo oceánico COAWST. Los resultados obtenidos del modelo se analizaron analítica y cuantitativamente. Luego se aislaron campos oceánicos sensibles a la fuerza del viento en los procesos costeros y los sistemas estuarinos. Los resultados permitieron percibir el impacto del viento en las corrientes oceánicas, en el intercambio entre aguas continentales y oceánicas (a través de la salinidad estratificada en la columna de agua) e impactos en los frentes costeros. La velocidad media del viento en los datos filtrados obtenidos disminuyó aproximadamente 2 m/s en todas las direcciones en comparación con la velocidad de los datos de resolución completa. Las diferencias más notables en la velocidad de flujo se observaron en sistemas de baja presión, obteniendo valores más precisos y consistentes en los datos filtrados. La herramienta de modelado creada se puede replicar y aplicar en diferentes regiones del mundo como un instrumento para comprender y mitigar los impactos marinos costeros.

Palabras Clave: Fuerza de viento, hidrodinámica, COAWST, HRRR, intercambio de aguas.

ABSTRACT

Mississippi Sound is a shallow water estuarine system separated from Gulf of Mexico shelf waters by barrier islands and characterized by its strong weather fronts, storms, and hurricanes that affect the hydrodynamic and morphological factors of the area. In this study, a numerical modeling system is used to study the effects of the wind on coastal settings, inlets, and water exchange. The present work developed a MATLAB computational algorithm that filters and interpolates the wind forcing file obtained through the High-Resolution Rapid Refresh (HRRR) product to model the two data sets (unfiltered and filtered) in the COAWST ocean model. The results obtained from the model were analyzed analytically and quantitatively. Oceanic fields that are sensitive to wind force in coastal processes and estuarine systems were then isolated. The results made it possible to perceive the impact of the wind on ocean currents, on the exchange of continental and oceanic waters (through stratified salinity in the water column) and impacts on coastal fronts. The mean wind speed in the filtered data obtained decreased by approximately 2 m / s in all directions compared to the speed of the full resolution data. The most notable differences in flow velocity were observed in low-pressure systems, obtaining more precise and consistent values in the filtered data.

The modeling tool created can be replicated and applied in different regions of the world as an instrument to understand and mitigate coastal marine impacts.

***Keywords**: Wind forcing, Hydrodynamics, COAWST, HRRR, Ocean exchange.*

TABLE OF CONTENTS

EVALUATION COURT 5
RESUMEN I
ABSTRACT II
TABLE OF CONTENTS III
ABBREVIATIONS V
LIST OF SYMBOLS VI
TABLE OF FIGURES VII
TABLE INDEX IX
CHAPTER 1 1
1 INTRODUCTION 1
1.1. Problem description 1
1.2. Problem justification 2
1.3. Objectives 4
1.3.1. General Objective 4
1.3.2. Specific Objectives 4
1.4. Literature review 5
1.4.1. Study Area 5
1.4.2. Ocean parameters 8
1.4.2.1. Salinity and Temperature 8
1.4.2.2. Waves 10
1.4.2.3. Tides 10
1.4.3. Winds 13
1.4.4. Currents 14
1.4.5. Impacts of extreme storms in the Mississippi Sound 15
1.4.6. COAWST 17
CHAPTER 2 20
2 METHODOLOGY 20
2.1 Data acquisition 22
2.2 Filter algorithm 23
2.3 COAWST Setup model 25
2.3.1 Data extraction for graphs creation 27
CHAPTER 3 29

3 RESULTS AND ANALYSIS 29
3.1 Study Area 29
3.2 Wind Rose 30
3.3 Surface Sea Temperature 33
3.4 Salinity in the water column 34
3.5 Temporal line for wind forcing data 34
3.6 Comparative standard deviation Hovmoller Plots 35
3.7 Standard deviation for u and v winds forcing vectors 36
3.8 Curl Wind – Hourly range 38
3.9 Sea Breeze Circulation Vs Land Breeze Circulation – Daily average 39
3.10 Costs Analysis 40
CHAPTER 4 41
4. CONCLUSIONS AND RECOMMENDATIONS 41
BIBLIOGRAPHY 44
APPENDIX 47

ABBREVIATIONS

ESPOL	Escuela Superior Politécnica del Litoral
USM	The University of Southern Mississippi
COAWST	Coupled Ocean-Atmosphere Wave Sediment Transport Modeling System
NOAA	National Oceanic and Atmospheric Administration
NDBC	National Data Buoy Center
HRRR	Hight-Resolution Rapid Refresh
ROMS	Regional Ocean Modeling System
MS	Mississippi Sound
AL	Alabama
LBC	Land Breeze Circulation
SBC	Sea Breeze Circulation
WRF	Weather Research and Forecast Model
SWAN	Simulating Waves Nearshore
RTG	Real Time Global
SST	Sea Surface Temperature
CDT	Central Daylight Time

LIST OF SYMBOLS

m	Meter
ft	Feet
in	Inches
h	hour
min	minutes
m/s	meters per second
U_{wind}, V_{wind}	Surface winds
P_{atm}	Atmospheric pressure
RH	Relative humidity
T_{air}	Atmospheric surface temperature
cloud	Cloud fraction
rain	Precipitation
SW_{rad}	Shortwave
LW_{rad}	Longwave
u_s, v_s	Surface currents
η	Free surface elevation
bath	Bathymetry
H_{wave}	Significant wave height
L_{wave}	Wavelength
D_{wave}	Wave direction
T_{surf}, T_{bott}	Surface and bottom periods
Q_b	Percent wave breaking
W_{dissip}	Wave energy dissipation
U_b	Bottom orbital velocity
ppt	parts per thousand

TABLE OF FIGURES

Figure 1.1 Area of studies and its estuarine areas of greater relevance [Google Earth]..5
Figure 1.2 Barrier Islands in the Mississippi Sound and associate inlets. Deep shipping channels are shown with white lines. (Morton Robert A., 2007) 5
Figure 1.3 Morphological change in Petit Bois Island between 1848 and 2005 (Morton Robert A., 2007) 7
Figure 1.4 Salinity estuarine zones in a long-term period, divided in 3 schemes: Tidal fresh zone, Mixing zone and Seawater zone. (Nelson, 2015).....8
Figure 1.5 Graphs of average salinity by season for the years 2000 to 2017 - Gulf of Mexico (Seidov et al., 2020) 9
Figure 1.6 Graphs of average sea surface temperature by season for the years 2000 to 2017 (Seidov et al., 2020)……..10
Figure 1.7 Mean Tidal Level in Dauphin Island for the dates 07/14/2016 14:000 to 08/01/2016 23:59 (NOAA, 2021).....12
Figure 1.8 Tide range vs Time for 30 days in January and June 2021 at Petit Bois Island, MS (NOAA, 2021) 12
Figure 1.9 Wind Rose from 00:00 January 1st, 2016, to 23:00 December 31st, 2016. Station: Keesler AFB/Biloxi, Mississippi. (Iowa State University, 2021).....13
Figure 1.10 Interconnected Ocean currents that intervene in the dynamics of the Gulf of Mexico. (Sanibel Sea School, n.d.) 14
Figure 1.11 historical land loss with respect to the presence of the most notable hurricanes in Mississippi Sound from 1850 to 2020 (Morton Robert A., 2007) 15
Figure 1.12 COAWST components for data exchange and increase of prediction and resolution.....17
Figure 1.13 Attributes exchange between models in COAWST (Warner John et al., 2010) 18
Figure 1.14 COAWST integrate an ocean model, atmospheric model, waves model, and sediment transport model using a Model Coupling Toolkit to exchange data between them. (Warner John et al., 2010) 19
Figure 2.1 Systematic methodology of the project next to the Design Thinking Methodology.....20
Figure 2.2 Solution proposal.....21
Figure 2.3 NDBC distribution map for the study area [NOAA] 22

Figure 2.4 Script used to filter and interpolate the wind forcing vectors 24
Figure 2.5 COAWST setup 25
Figure 2.6 Bash file modification 26
Figure 2.7 End of COAWST configuration 27
Figure 3.1 Magnified view of the study area made using QGis 29
Figure 3.2 Georeferencing of the study area, barrier islands, and inlets with which we work on the project. 30
Figure 3.3 Mooring locations that were used for the generation of wind roses. Data were acquired from the National Data Buoy Center archives (NDBC) 30
Figure 3.4 Sea Surface temperature for July 29th, 2016, at 11 UTC (left) and at 20 UTC (right) 33
Figure 3.5 HRRR vs HRRR24 comparison for Standard deviation and Mean Salinity values in the water column in West Ship Pass 34
Figure 3.6 Wind filter data Vs Wind Unfiltered data - Main Pass 35
Figure 3.7 Comparison for "v" current velocity between filter and unfiltered data for Horn Island Pass 36
Figure 3.8 Comparison for "u" current velocity between filter and unfiltered data for Horn Island Pass 36
Figure 3.9 Standard deviation of u current velocity vectors for the entire two weeks in Horn Pass only for Land Breeze and Sea Breeze Circulation periods 37
Figure 3.10 Standard deviation for v (northward) current velocity in the water column - Cat Pass over the entire 2-week only for Land Breeze and Sea Breeze Circulation periods period 38
Figure 3.11 Wind and v (northward) current velocity circulation for Cat Pass on July 15, 2016 at 00:00 UTC 39
Figure 3.12 example two of Wind and v (northward) current velocity circulation for East Ship Pass on July 21, 2016, at 17:00 UTC 39
Figure 3.13 Sea and Breeze circulation snapshot for Cat Pass: 07/16/2016 at 1100 UTC 40

TABLE INDEX

Table 1.1 Comparison of the three reanalysis products.....3
Table 1.2 Historic hurricanes in the northern Gulf of Mexico and parameters to evaluate storm effects. (Morton Robert A., 2007) 16
Table 3.1 Wind Roses at NDBC's locations for HRRR unfiltered and filtered outputs ...31
Table 3.2 Cost analysis 40

CHAPTER 1

1 INTRODUCTION

1.1. Problem description

Mississippi Bight is constantly threatened by marine pollution problems, high risk of hurricanes, storms, flooding caused by overflowing rivers and reservoirs, and droughts at certain times of the year. These threats gravely affect the populations of flora and fauna of the marine ecosystem, to the point of making them disappear or forcing them to migrate to distant waters. Consequently, the economy of society also declines, causing a chain of unfortunate events. (Moncreiff Cynthia A. et al., 2007) Furthermore, its shallow depth is also a problem; the average depth of the study area is 4 m, with certain exceptions in the navigation channels and deep-water ports located in Gulf Port and Pascagoula, where the depth reaches 12 m (Hossain et al., 2019). Due to its shallow depth, the impacts from natural disasters as hurricanes or storms affect and interfere with the hydrodynamics and morphodynamics of the area. Concerning hydrodynamics, the risk factors are the flow pattern, current velocity, waves, erosion, sedimentation, and circulation in 3 dimensions of water. In the Gulf of Mexico area, the significant wave height is generally less than 1 m (Hwang et al., 1998), and in the coastal area of Mississippi, there is only one high tide and low tide during the day with fluctuations of +- 0.50 m. For this reason, the wind is the primary conductor of currents and is responsible for the exchange of ocean and continental waters.

Therefore, it is necessary to study the effects of wind on complex scenarios, inlets, ocean exchange, and estuarine dynamics through a graphic model. To achieve this requires a model that provides high spatial and temporal resolution of wind force to resolve atmospheric circulation over the complicated features of the Mississippi Sound area's coast lines.

1.2. Problem justification

The Mississippi Sound is characteristic for presenting complex scenarios on its coasts, which are strongly affected by atmospheric circulation. The present work is part of a much larger-scale research project in which they have managed to model wind speed patterns to determine their effects on the coastal zone. However, some of the components used in modeling are no longer available; therefore, the modeling will have to be carried out in a new element for future research. In this project, this new component is validated, and modifications are made that will improve it to be used in future modeling for the benefit of oceanic, coastal, and estuarine well-being.

The Ocean Modeling Group at the University of Southern Mississippi (USM) developed a high spatial resolution (400-m) application of the coupled ocean-atmosphere wave sediment transport modeling system (COAWST) with the Regional Oceanic Modeling System (ROMS.) at its core during the CONCORDE project (Consortium for Coastal River Dominated Ecosystems) (Greer et al., 2018) funded by the Gulf of Mexico Research Initiative (GoMRI). (Armstrong B. N. et al., 2021)

The COAWST-based coupled model system has been used to run simulations from 2015 to 2017 using three different atmospheric forcing products; one is the North American Regional Reanalysis (NARR); the second is the CONCORDE Meteorological Analysis (CMA) product, and from 2018 and into the future, they are applying the High-Resolution Rapid Refresh (HRRR) as atmospheric forcing. The coupled model system is being used to help us better understand the dynamics and physical drivers of freshwater transport in this region and the impact of freshwater inflow from regional rivers and diversions. (Armstrong B. N. et al., 2021)

CMA is the highest resolution wind forcing product at hourly 1-km resolution, but as this is no longer available, we decided to use the second highest, which is HRRR. This product features an hourly temporal resolution with a 3 km spatial

resolution. Table 1.1 details the main characteristics of the three wind products considered in the design.

This work examines two runs in a set of numerical experiments using HRRR as the atmospheric forcing product. These experiments are being performed to provide insight into the need for well-resolved forcing in coastal ocean modeling applications realizing inlet exchange and estuarine dynamics. By comparing full resolution and filtered wind forcing, we can isolate changes in ocean circulation resulting from increased temporal resolution in the wind forcing field.

Table 1.1 Comparison of the three reanalysis products

	CMA CONCORDE Meteorological Analysis	**HRRR High Resolution Rapid Refresh**	**NARR North American Regional Reanalysis**
Temporal resolution	Hourly	Hourly	3-Hourly
Spatial resolution	1-Km	3-Km	32-Km
Product type	Gridded meteorological reanalysis product	Weather Research and Forecast -WRF model product	Reanalysis product

1.3. Objectives

1.3.1. General Objective

Study the ocean response to the impact of wind on the hydrodynamics and morphodynamics of marine-coastal areas in the Mississippi Sound region.

1.3.2. Specific Objectives

- Develop an algorithm for filter and interpolation of wind forcing files.
- To model the two wind forcing sets in COAWST.
- To graphically represent modeled results.
- Compare results obtained from unfiltered and filtered wind forcing files.
- Isolate and qualitatively and quantitatively analyze the differences between both models.
- Find areas of greater vulnerability to the impact of the force of the wind.
- Verify that the high-resolution HRRR product is the most appropriate and accurate for conducting modeling studies in the Mississippi Sound

1.4. Literature review

1.4.1. Study Area

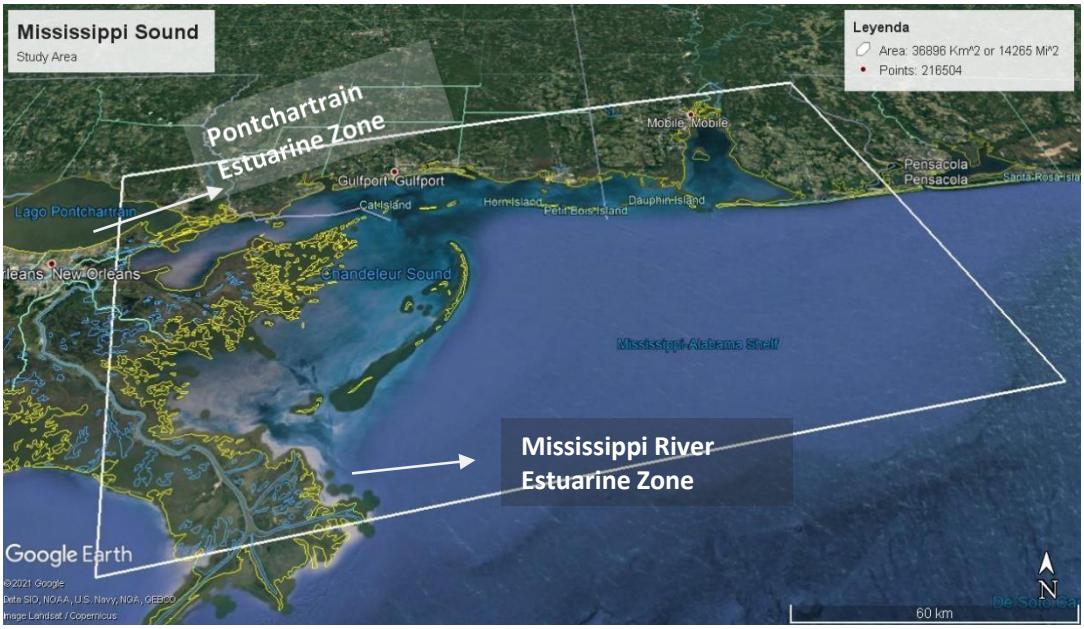

Figure 1.1 Area of studies and its estuarine areas of greater relevance

[imagen from Google Earth]

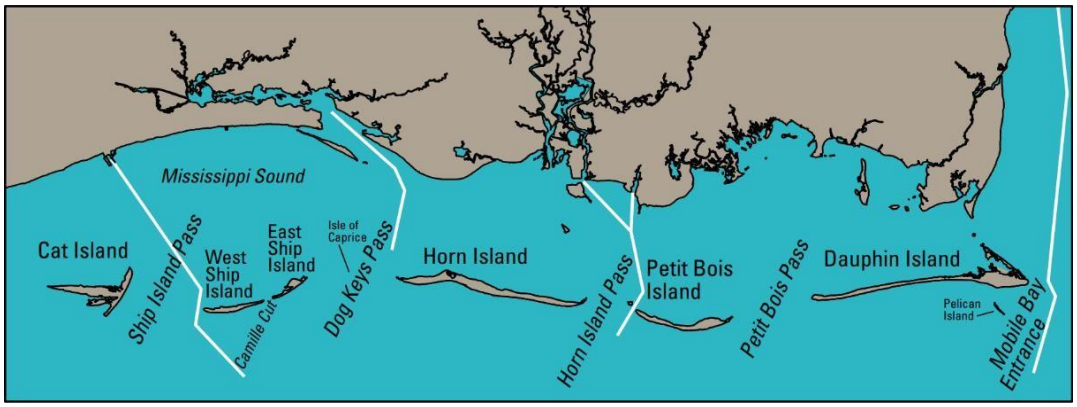

Figure 1.2 Barrier Islands in the Mississippi Sound and associate inlets. Deep shipping channels are shown with white lines. (Morton Robert A., 2007)

Mississippi Sound is constituted of the shallow waters along the shores of Alabama, Mississippi, and Louisiana (Figure 1.1). It has a surface area of 4792 km^2, its average daily freshwater flow is 1234.61 m^3/s, which mainly sources from the Pearl and Pascagoula Rivers. The estuarine waters of MS are separated from the continental shelf (MS Bight) and the Gulf of Mexico proper by five barrier

islands (Figure 1.2): Cat, Ship, Horn, Petit Bois and Dauphin (U.S. Fish and Wildlife Service., 1982) .

The barrier island chain is located north of the inner continental shelf adjacent to the northern Gulf of Mexico and extends from Mobile Bay in Alabama to Atchafalaya Bay in Louisiana. These islands are losing soil due to sediment transport and rising sea levels (Figure 1.3). However, this loss of soil is expected behavior because the conditions in which the islands were created are not the same as the current conditions; An example of this is the constant rise in sea level over thousands of years, there is also a more usual presence of hurricanes and increasingly energetic winter storms capable of definitively removing sediments from the islands. These effects act in equal measure on the beaches and the coastal surface, increasing their erosion rate. (Morton Robert A., 2007)

The Intracoastal channel of the MS has an average depth of 4 m, while the fluvial channel built for the transit of tugs and barges has a depth of 6 m. The western section of Cat Island and the northern section of Dauphin Island depend on continuous maintenance dredging by the coast guard (Morton R., 2007). The estuaries of the area are constantly threatened by natural events, including floods from rivers and reservoirs. In 2008 and 2011, the floodgates of the Bonnet Carré Spillway were opened, which caused the destruction of the oyster and crab populations, which the authorities tried to remedy by cultivating these species as a medium-term remediation method (Morton R., 2007).

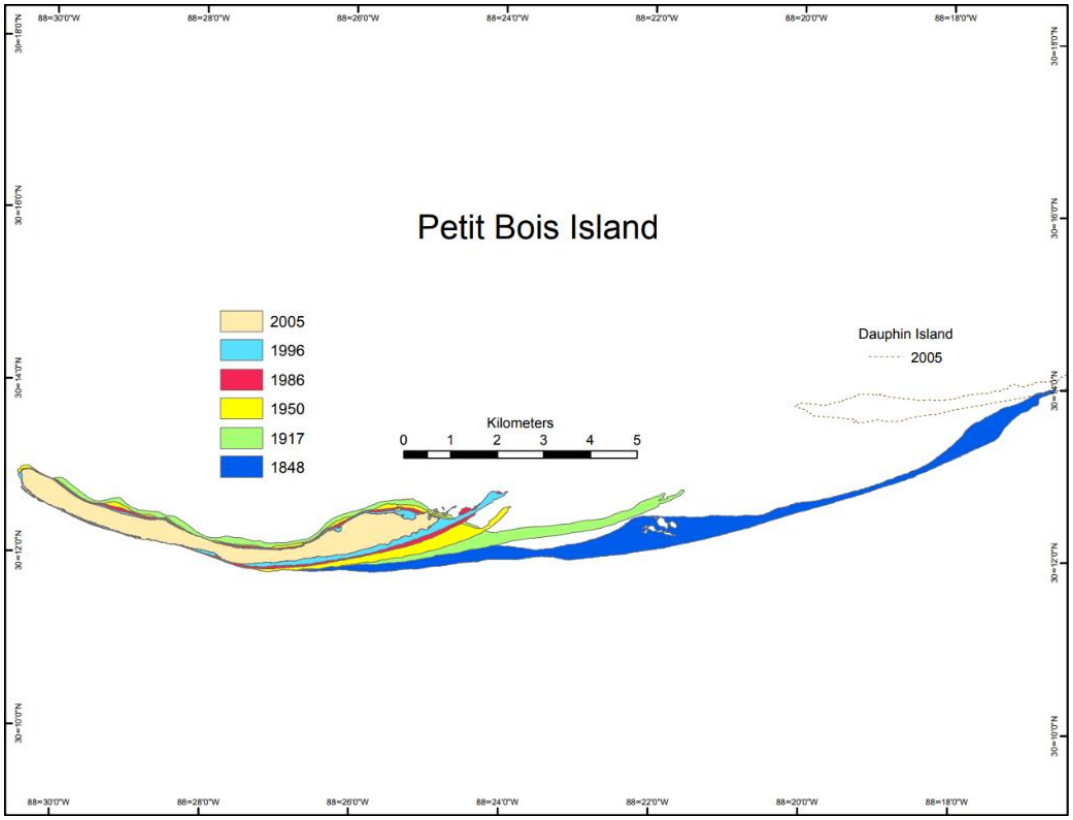

Figure 1.3 Morphological change in Petit Bois Island between 1848 and 2005

(Morton Robert A., 2007)

1.4.2. Ocean parameters

1.4.2.1. Salinity and Temperature

The estuarine zones are a fundamental aspect of our investigation; its salinity is considered static because it does not have a remarkable seasonal variation in its patterns (Nelson, 2015). In Figure 1.4, we can see the mixing zone between seawater and freshwater:

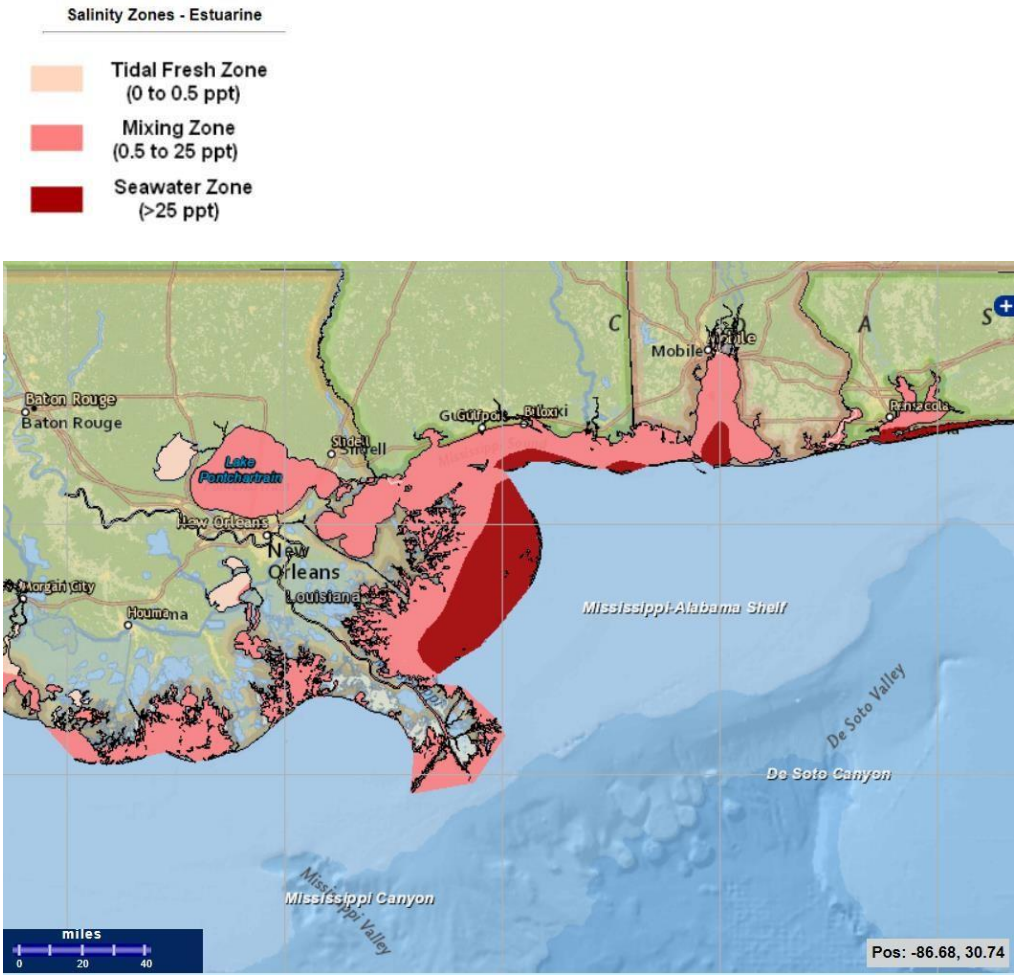

Figure 1.4 Salinity estuarine zones in a long-term period, divided into 3 schemes: Tidal fresh zone, Mixing zone and Seawater zone. (Nelson, 2015)

Salinity north of the Gulf of Mexico varies by season of the year. Mississippi has four seasons which are winter, spring, summer, and fall (Figure 1.5 and 1.6). Winter (January to March) is a cold season with an average SST of 18°C and salinity between 32 to 34. Spring (April to June), the average SST is 24°C, and its salinity ranges between 34 and

35. Summer (July to September) is the hottest season, it has an average SST of 29°C, and its salinity maintains values of 34. The last season of the year is fall, between October to December; this is a warm season with an average SST between 22°C to 24°C; the salinity of the station is 35.

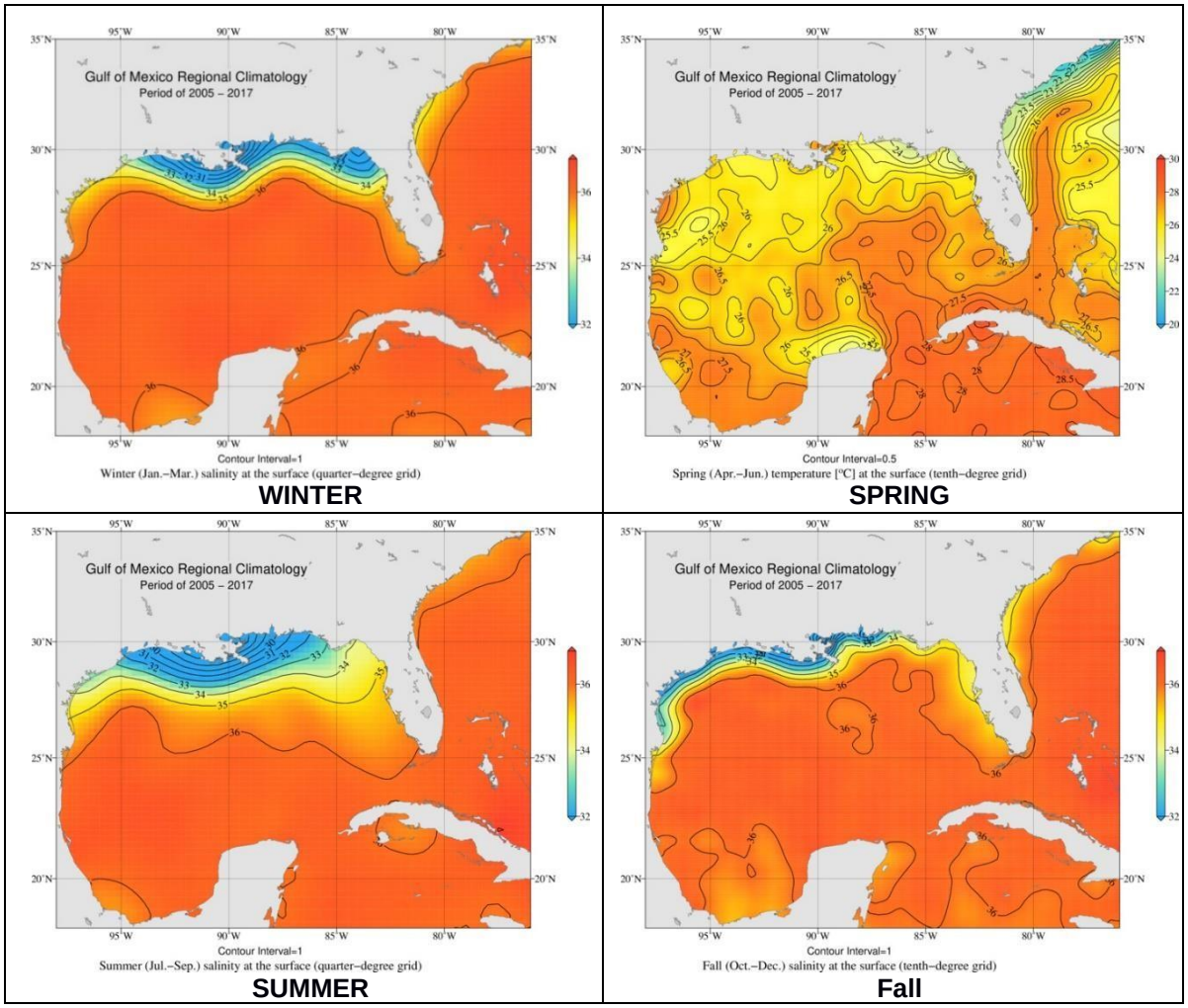

Figure 1.5 Graphs of average salinity by season for the years 2005 to 2017 - Gulf of Mexico (Seidov et al., 2020)

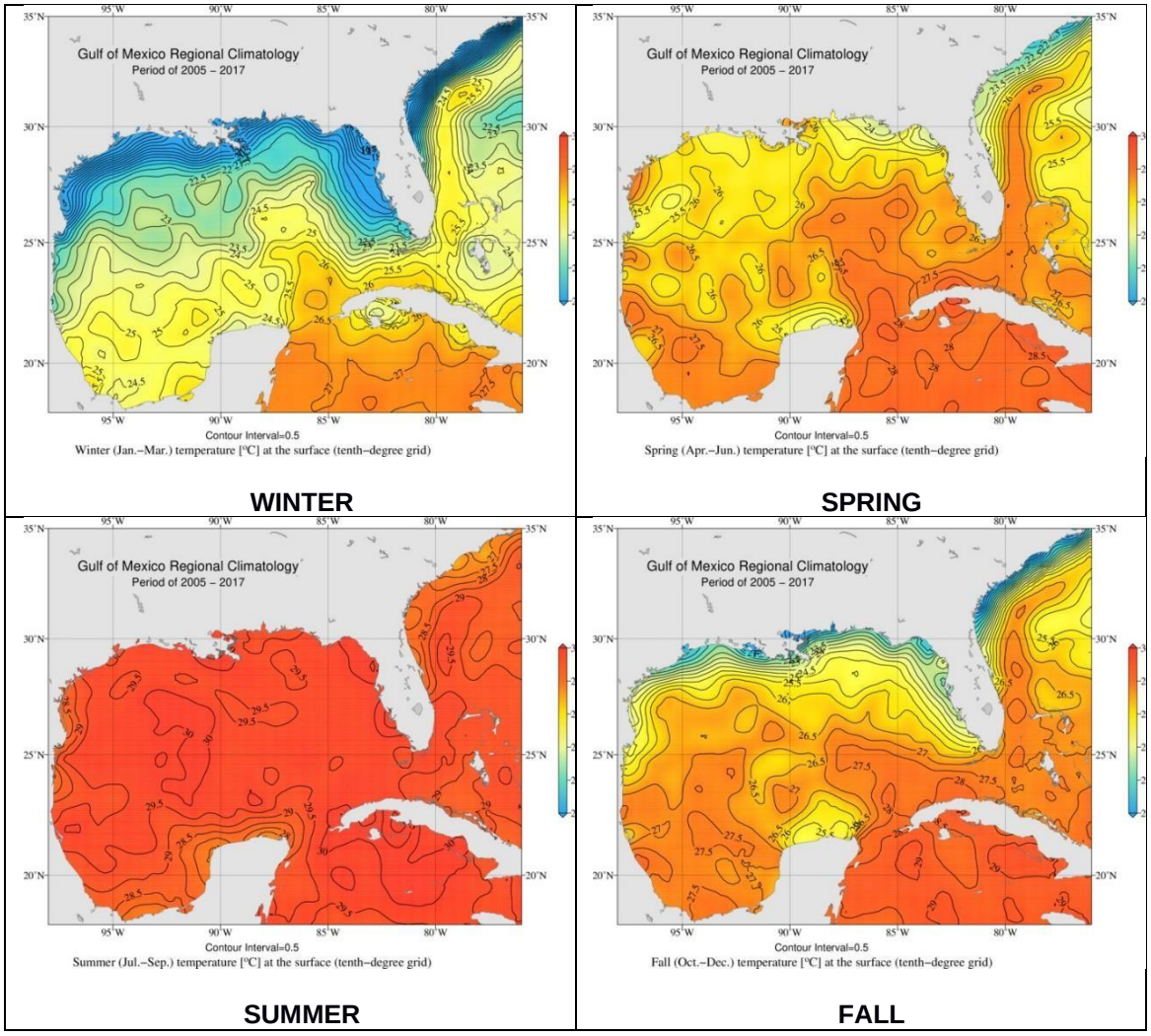

Figure 1.6 Graphs of average sea surface temperature by season for the years 2005 to 2017 (Seidov et al., 2020)

1.4.2.2. Waves

The average wave height in the southern part of the barrier islands is 0.4 to 0.8 m with a wave period of 5 s. when the waves enter through the inlets towards the coast, they lose energy, and their average height is from 0.1 to 0.3 m with a period of 2 s. (NOAA, 2021)

1.4.2.3. Tides

The tides of the MS are diurnal; namely, there is a high tide and a low tide during the day. Figure 1.8 is the tidal range for January and June 2021; in this

graphic can be seen that for each day, the tide presents a high tide and a low tide, high tide generally occurs during the day, and low tide occurs at night. In addition, the month of June shows a higher tidal height (0.2 m) about January; however, both months show a very similar harmonic curve. The platform currents involved in the tides are Sverdrup waves with typical velocities of 5 to 10 cm/s. (Seim et al., 1987) The tides lose height and energy when passing through the inlets of the barrier islands. For example, in Figure 1.7 on July 15th, 2016, the tides reached Dauphin Island with an average height of 0.5 m, and after passing through the inlets, its height decreased to 0.2 m on average. (NOAA, 2021)

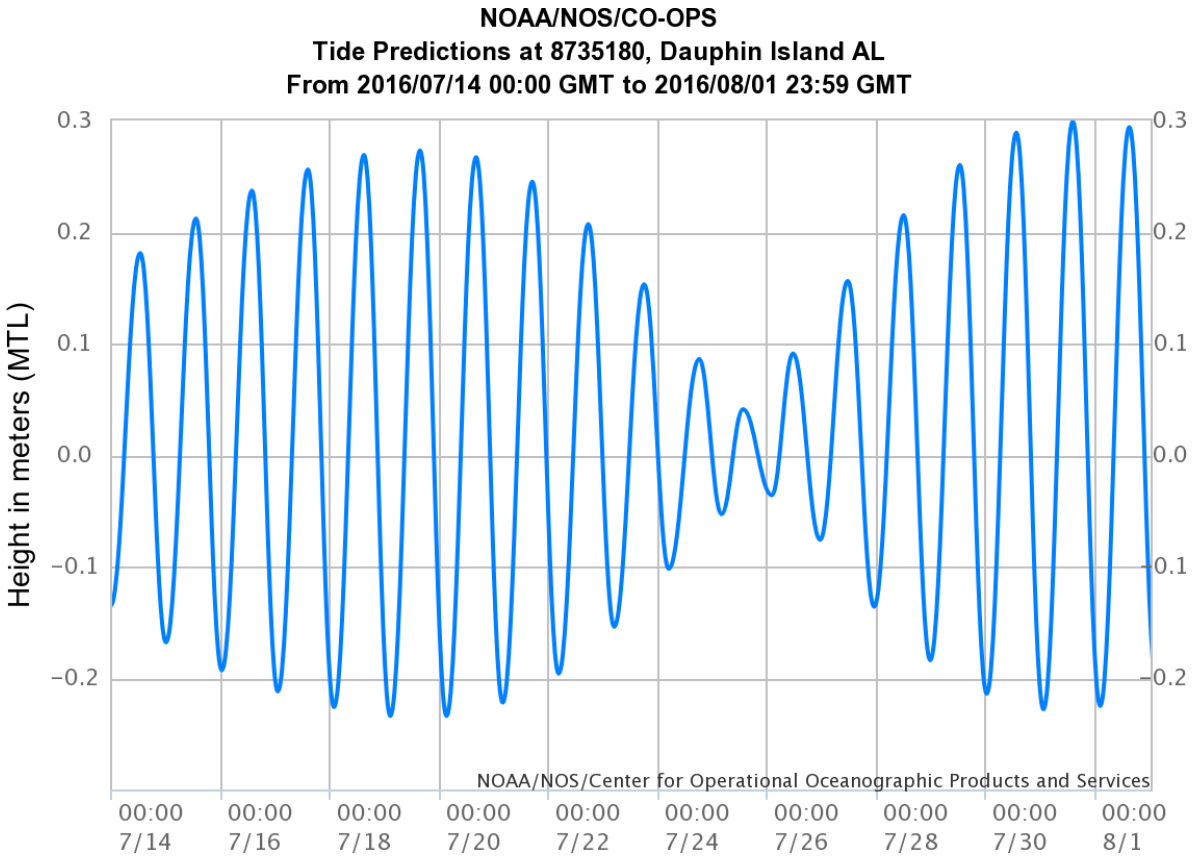

Figure 1.7 Mean Tidal Level in Dauphin Island for the dates 07/14/2016 14:000 to 08/01/2016 23:59 (NOAA, 2021)

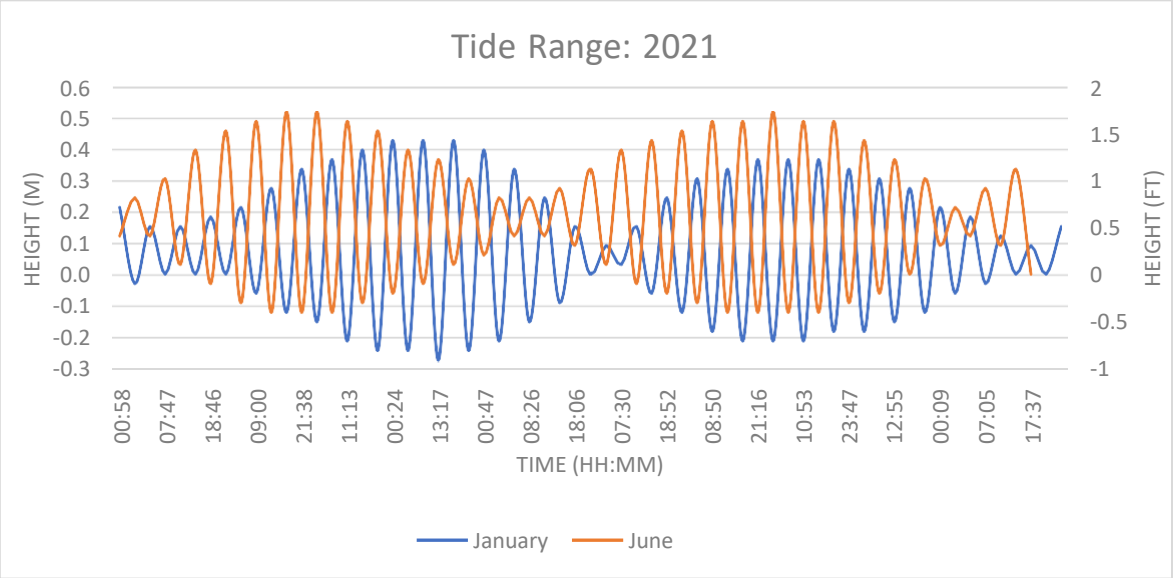

Figure 1.8 Tide range vs Time for 30 days in January and June 2021 at Petit Bois Island, MS (NOAA, 2021)

1.4.3. Winds

The tidal range in the MS and throughout the Gulf of Mexico does not go beyond 0.5 m; therefore, the primary mechanism in erosion and sediment transport is the waves generated by wind and currents. In the Gulf, easterly winds predominate for most of the year, causing coastal currents to head west (Curray & Moore, 1963). These coastal currents are reinforced by the wind circulation in the opposite direction to the clock's hands, also associated with tropical cyclones. Hurricanes and tropical storms head toward the coast of MS and AL, moving north or west and creating wind patterns directed from the east. The combination of wind strength and wave intensity forms currents that can erode and transport large volumes of sediment in short periods, altering the area's morphology. The impact of sediment erosion on the islands depends on the height and direction of storm surges and shoreline elevations. (Morton Robert A., 2007)

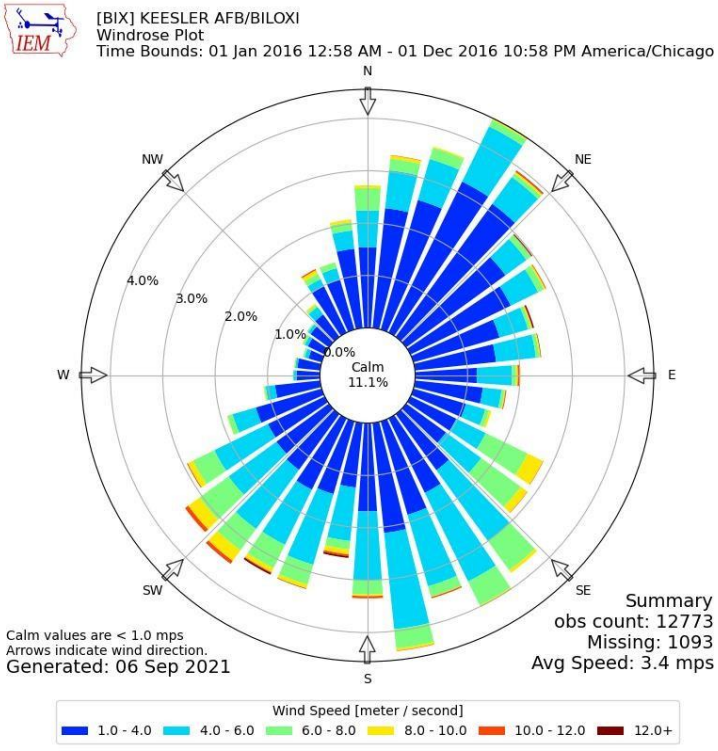

Figure 1.9 Wind Rose from 00:00 January 1st, 2016, to 23:00 December 31st, 2016. Station: Keesler AFB/Biloxi, Mississippi. (Iowa State University, 2021)

1.4.4. Currents

The Gulf is dominated by a singular current known as the “Loop Current.” (Figure 1.10) It begins as the “Yucatan current,” entering the Gulf of Mexico from the southeast, passing the Yucatan peninsula before moving clockwise along the coast, exiting the Gulf as the “Florida current.” This current is prone to producing anti-cyclonic eddies, which often happens when the current “intrudes” toward the middle of the Gulf rather than along the coastal regions. In this scenario, warm eddies are shed, which move toward the western Gulf. These eddies tend to be larger than 300km in diameter but can be as small as 150km and are the primary mover of water throughout the Gulf. These “shedding” takes between 3-17 months to run their course, and these eddies create implications among other weather patterns and human activity. With severe eddies and surges, offshore drilling operations may be put at risk. Also, large eddies can result in severe hurricane intensification when both forces reside in the same region, as was the case with Hurricane Opal. (Kantha L. et al., 1999)

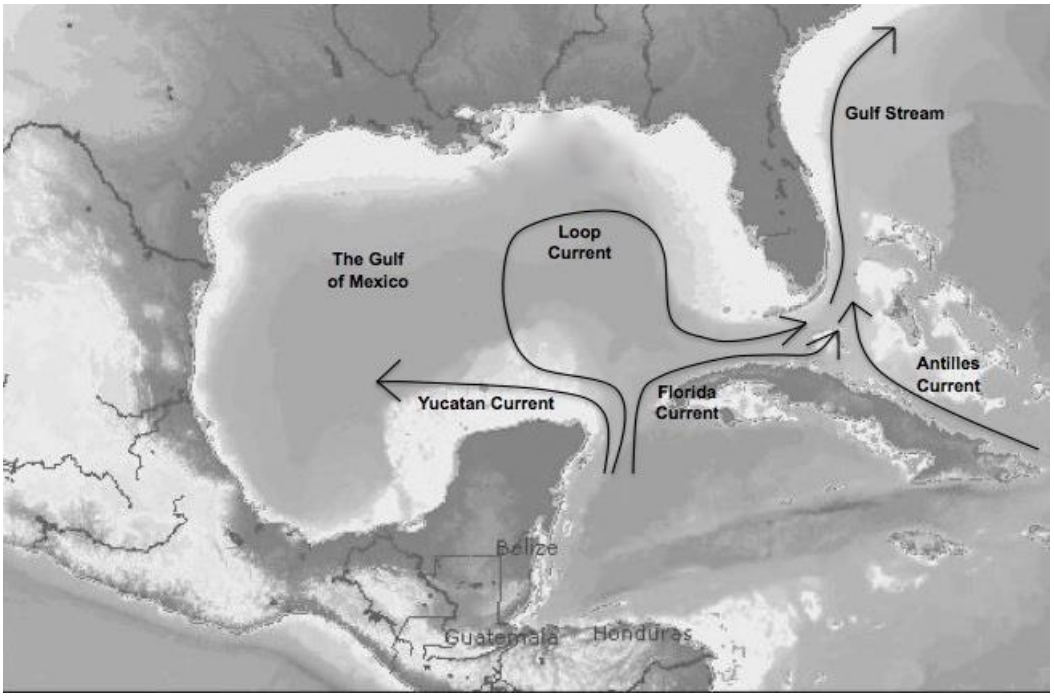

Figure 1.10 Interconnected Ocean currents that intervene in the dynamics of the Gulf of Mexico. (Sanibel Sea School, n.d.)

1.4.5. Impacts of extreme storms in the Mississippi Sound

Storms are a disturbance in the atmosphere resulting in high winds, rain, and low pressure (Vitart et al., 1997). The typical path that tropical cyclones follow when entering the Gulf of Mexico makes the north coast between Florida and Louisiana have a high incidence of storm impacts. The waters of Mississippi Sound have recorded numerous hurricanes since 1800 (Morton, 2003). Figure 1.11 details the morphological changes of the islands due to the passage of these hurricanes.

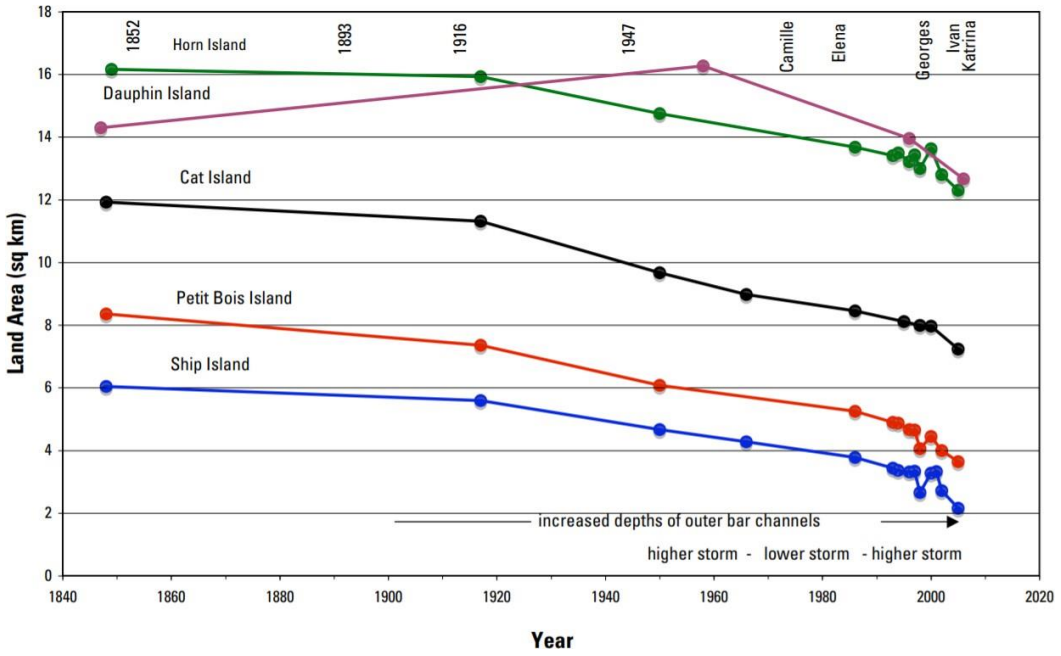

Figure 1.11 Historical land loss to the presence of the most notable hurricanes in Mississippi Sound from 1850 to 2020 (Morton Robert A., 2007)

Hurricane Katrina was a vast and powerful hurricane that delivered great destruction along the Gulf Coast, providing tropical force winds and rain to much of the southeast. On August 28th, 2005, Katrina reached peak intensity with hurricane-force winds stretching 170km from the center and tropical-storm-force winds stretching 370km from the center (Knabb et al., 2005). Although Katrina weakened some from this peak intensity when it made landfall on August 29th, the size and strength of these winds were mainly maintained, leading to rapid destruction along the coast. The coastal areas of Louisiana and Mississippi are already prone to flooding as the lowland coastal plains lack barriers to storm surge and are just above or even below sea level, in the case of New Orleans

(FEMA, 2006). Storm surge was most remarkable along the eastern portion of Katrina's path, with 7-10 m of storm surge being the norm and surged penetrating as deep as 10km inland along the Mississippi plains (USACE, 1969). The Barrier Islands (Figure 1.2) experienced storm surge between 5.5-9m, and permanent changes were made to the islands because of the hurricane. High water levels engulfed the island for over a day, leaving salt burns on trees, snapping others in half, and eroding the coastline. With the death/reduction of foliage and tree cover on the edges of these islands (in particular Dauphin Island), erosion accelerated since no root systems held the land in place, leading to permanent land loss and widening of the channels between the islands (Schmid K., 2000). As a direct result of this storm, the barrier Islands became less of a barrier for oncoming storm surge and flooding to the Mississippi coast and provide even less protection today. (Fritz et al., 2007)

Table 1.2 describes the most destructive hurricanes and morphological effects that have been recorded in the area and its proximity to the MS barrier islands. This data is available in the archives of the National Hurricane Center. (Morton Robert A., 2007)

Table 1.2 Historic hurricanes in the northern Gulf of Mexico and parameters to evaluate storm effects. (Morton Robert A., 2007)

Year	Storm name	Intensity category	Eyewall proximity	Max. Water level (m)	Max. Windspeed (km/h)	Shelf Duration (h)
1916	Unnamed	3	Crossed Horn	2.3	195	36
1947	Unnamed	1	Passed south	3.6 - 4.2	150	30
1960	Ethel	5	Crossed Ship	1 – 1.5	260	24
1969	Camile	5	10-40 km westward	4.5 – 4.9	305	48
1985	Elena	3	Crossed Horn	1 – 2	185	103
1998	Georges	4-2	Crossed Ship	1.5 – 3	198	80

2004	Ivan	4-3	70-130 km east	1.5	120	54
2005	Katrina	5-3	50-130 km west	5.6 - 7.6	150 - 185	78

1.4.6. COAWST

Coupled Ocean-Atmosphere-Wave-Sediment Transport (COAWST) is a high-resolution modeling system that is composed of other numerical models using a Model Coupling Toolkit (MCT) for the exchange of data between those described in Figure 1.12:

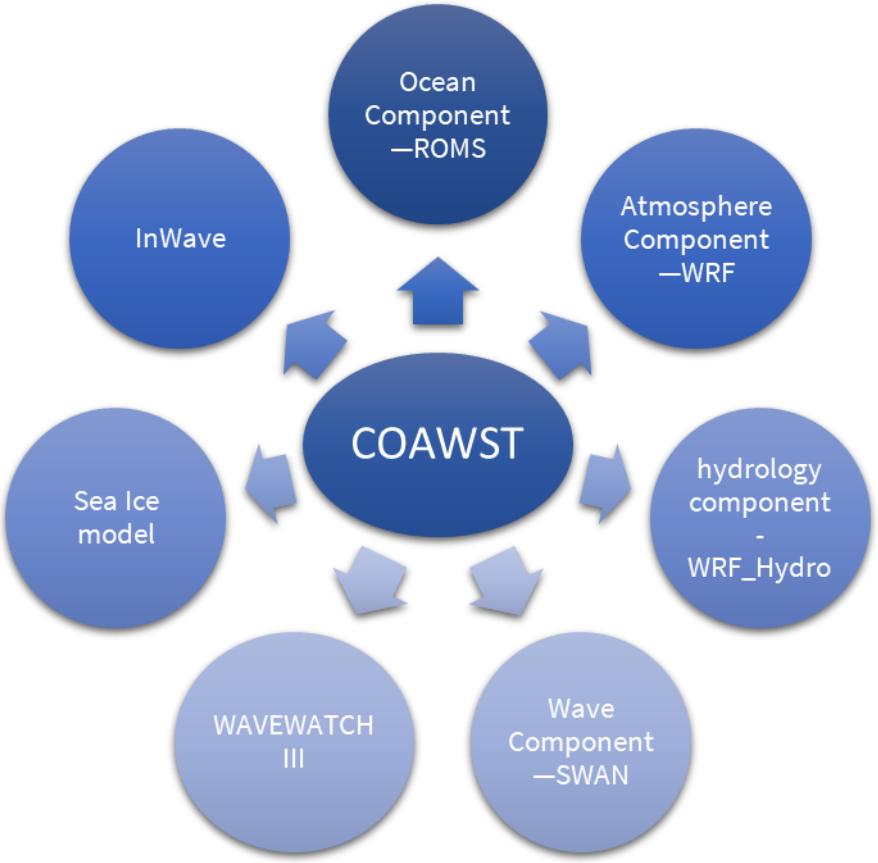

Figure 1.12 COAWST components for data exchange and increase of prediction and resolution

At startup, each processor of the models is compiled with MCT, which determines the distribution in the grid. Each model then fills its vector with attributes (forecast variables) to be exchanged with the other models (Warner John et al., 2010).

Figure 1.13 shows the variables that exchange:

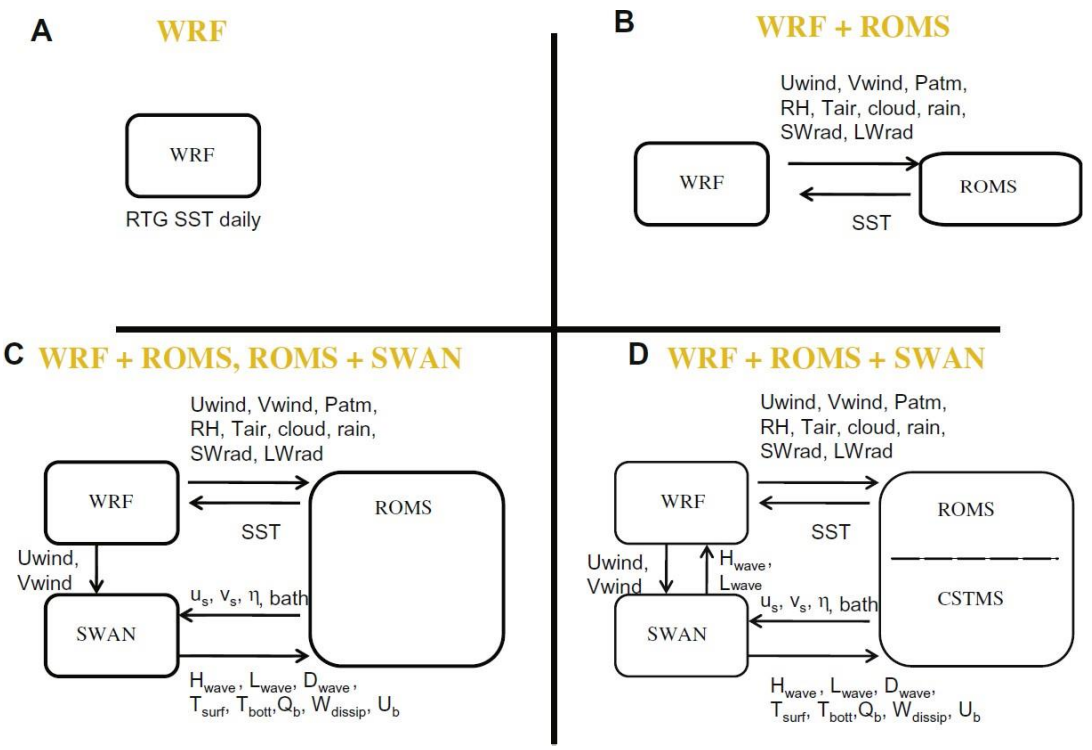

Figure 1.13 Attributes exchange between models in COAWST (Warner John et al., 2010)

There are currently many numerical models for predicting natural events. However, COAWST not only offers a high spatial and temporal resolution, but the coupling of other models makes this a versatile system capable of simulating complex scenarios to give an accurate approximation to natural events.

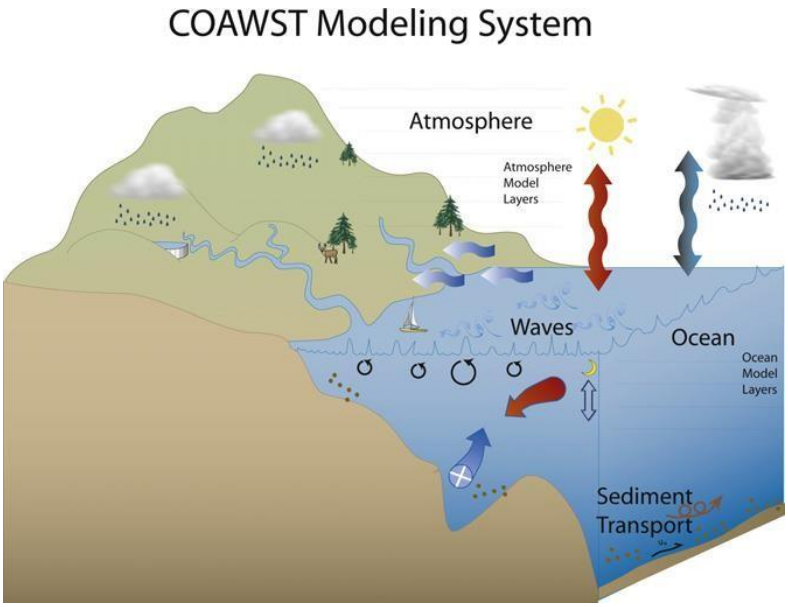

Figure 1.14 COAWST integrate an ocean model, atmospheric model, waves model, and sediment transport model using a Model Coupling Toolkit to exchange data between them. (Warner John et al., 2010)

CHAPTER 2

2 METHODOLOGY

The simplified methodology of the project is explained graphically in the following flow diagram:

Figure 2.1 Systematic methodology of the project next to the Design Thinking Methodology

The solution proposal of this project is based on the creation of a computational algorithm (Appendix A) that allows filtering the full resolution wind forcing provided by the University of Southern Mississippi (USM) and then applying that forcing to an oceanic coastal model, which enables the observation of the wind impact on coastal fronts, inlets, dynamics of estuarine systems and exchange between maritime and continental waters. From this observation, a comparison was made between the results forced by the full resolution wind data and the filtered wind data results. As a final step, the observed changes in ocean circulation were isolated, including variations in salinity and temperature in the water column resulting from the increase in temporal resolution in the wind force files. A simplified scheme of the methodological process can be seen in Figure 2.2:

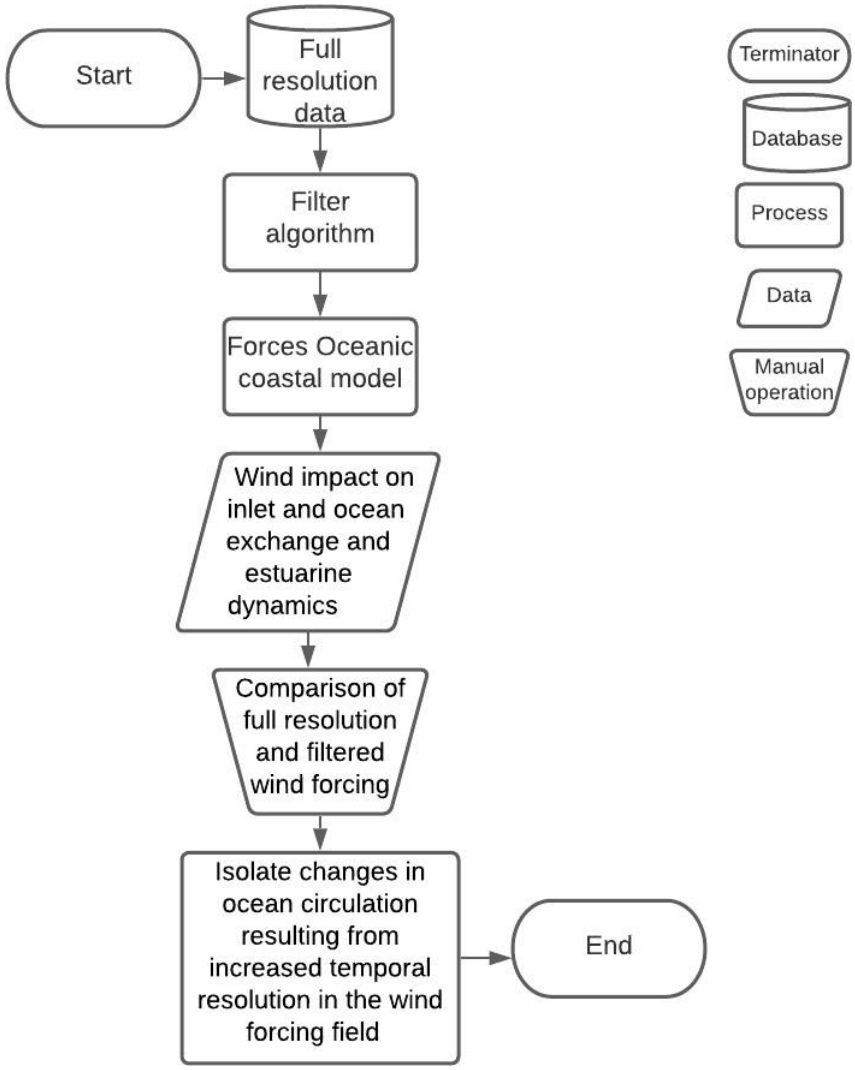

Figure 2.2 Solution proposal

For the development of this solution, a series of tools are required that were used throughout the project; these tools are listed below:

- Climatic information of the study area
- Oceanographic information of the study area
- Historical information of extreme events in the study area
- Data wind forcing files
- Computational algorithm - filter
- COAWST model
- Data extraction for graph creation

The historical oceanographic and climatic information was obtained through bibliographic references cited in the literature review.

2.1 Data acquisition

These complete resolution data upon which we will apply our digital filter were provided by USM, who extracted them from the official website of the University of Utah (Blaylock et al., 2018); this page is freely accessible thus everybody can download meteorological information at a global level for different periods and times of the year. The HRRR is an output collection obtained from the National Center for Environmental Prediction-NCEP's HRRR model, which is developed by NOAA ESRL and is run operationally hourly at NCEP's Environmental Modeling Center (Blaylock et al., 2017; Dougherty, 2020; Gowan, 2021). This information can also be corroborated by buoys placed on site by the National Data Buoy Center (NDBC) that take values of different variables from the points marked in Figure 2.3.

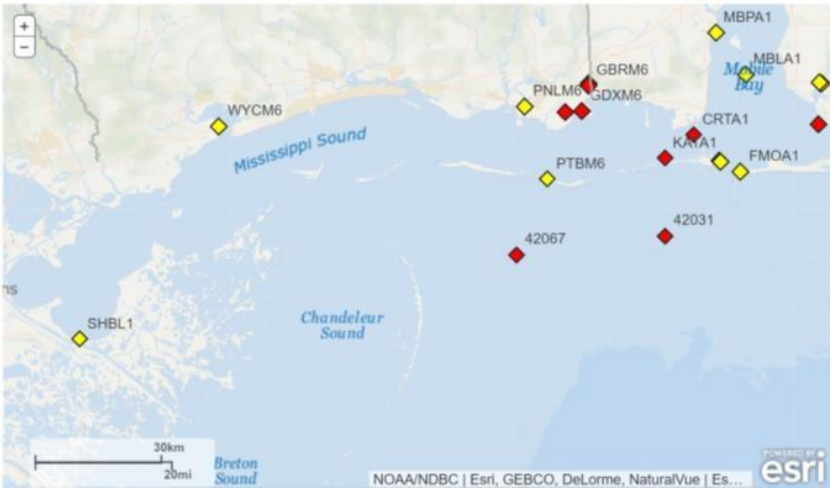

Figure 2.3 NDBC distribution map for the study area [NOAA]

2.2 Filter algorithm

MATLAB software was used for the development of this script. All the folders and files used in the routine must be placed in the same directory. Once the working directory is established in the code, the next step was calling the file that contains the wind forcing information; this file will have a Network Common Data Form (NetCDF) (Boulder, 2020) ".nc" file type; therefore, the MATLAB NCread function will be applied to extract the information found in the file. Once inside the file, we determine which variables are the ones we will use. The next step is to call the variables of the wind vectors in u and v directions. It should be clarified that the vector u is directed towards the east, while the vector v is directed towards the north. Consequently, it is possible to have negative values, which refer to the wind heading towards the west in the case of -u or towards the south in the case of -v.

To visually understand the distribution of our study area, we extracted the latitude and longitude variables. This data was placed in a matrix and transferred to an Excel file of comma-separated values (CSV) allows it to be read by QGIS and this, in turn, places it on the map according to the exact coordinates. The lowpass digital filter function requires entering a series of input data. Therefore, the number of data obtained for each day is extracted, which is one data point per hour; thus, there are 24 data points per day. In addition, we calculated the number of time steps; these are the total amount of data that the filter will work with. The other input data is the matrix with wind force and matrix dimension.

Finally, we apply the lowpass filter; this function transmits low frequencies while eliminating high frequencies creating a smoother pattern of data while interpolating data that have short spacing from each other and exclude data whose undetermined data-to-data values are much longer. The output file for this algorithm is a matrix with the same dimensions as the original file. The script process step by step is shown in the following scheme Figure 2.4:

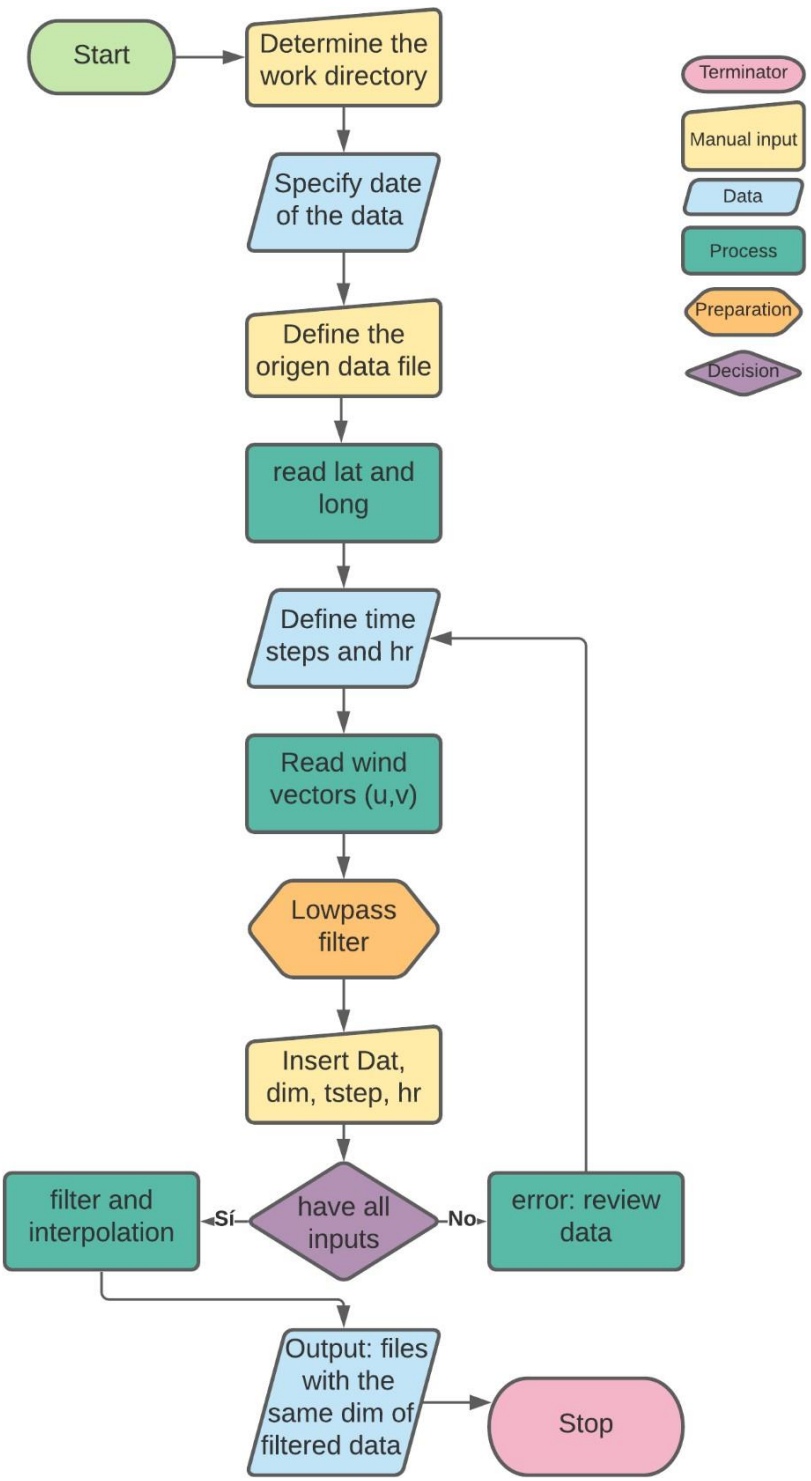

Figure 2.4 Script used to filter and interpolate the wind forcing vectors

2.3 COAWST Setup model

COAWST is a program for the modeling of oceanographic, coastal, and atmospheric characteristics. This program does not have a graphical interface; however, this does not impede working on it. Its use and handling are simple once we connect to the interface; in addition, the steps to apply are mechanical and easy to remember. Of course, like any other program, it also requires logic and analysis to develop models.

The modeling of the wind forcing in COAWST began with the configuration of the program. As a first step, it is advisable to open the program in a Linux operating system; then, we enter the folder that contains the HRRR product and the files to be modeled. The initial setup will be done in the "bash" file. To get access to it, we used the nano function as shown in Figure 2.5:

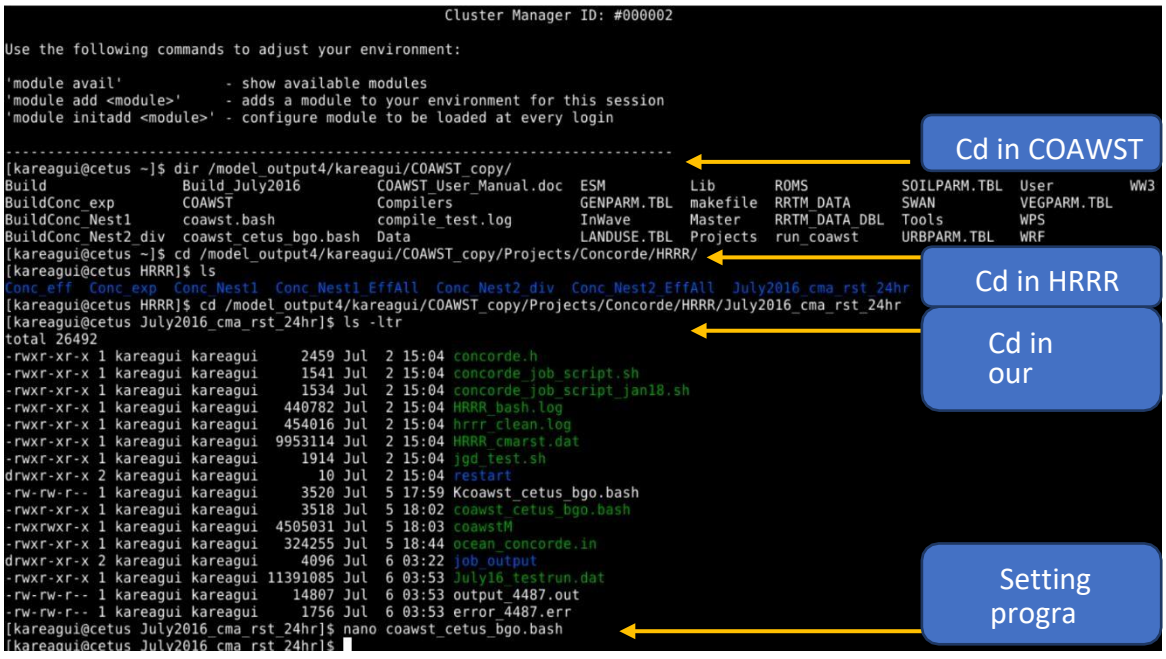

Figure 2.5 COAWST setup

Within the "bash" file, the root directory where all the necessary files are found, the directory where the project will be located, the input files, and the boundary conditions were selected. The other options will stay the same for default. This step is described in Figure 2.6:

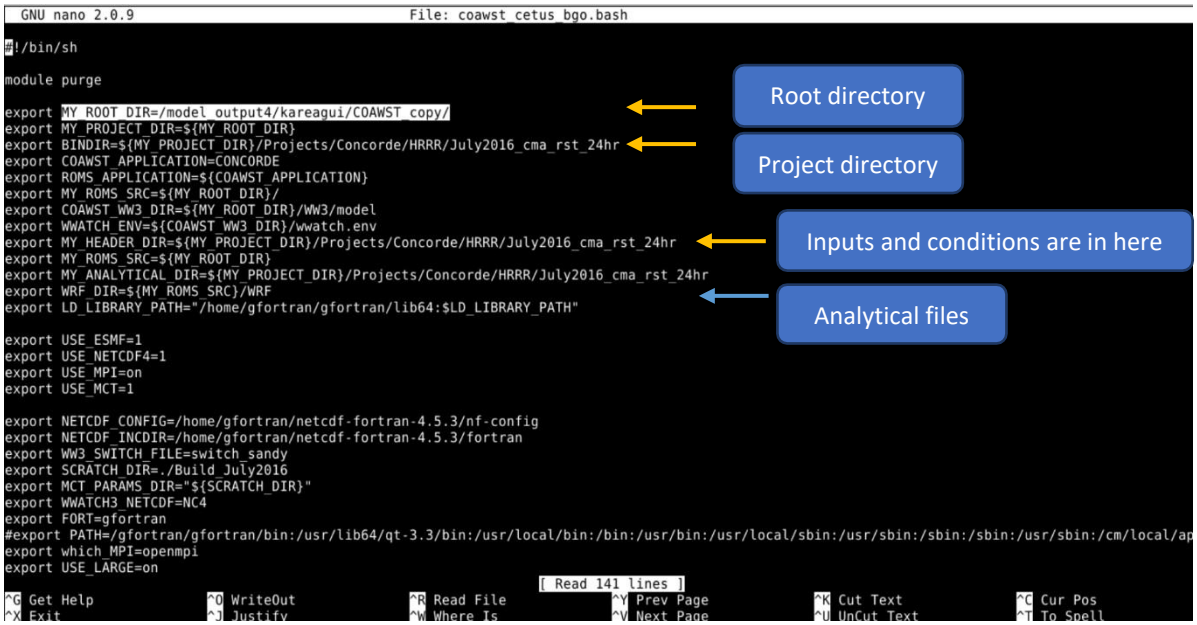

Figure 2.6 Bash file modification

The next step in Figure 2.7 was to compile this modified file. Then through the nano function, we accessed the file "ocean_concorde.in", here the initial conditions were edited, such as time step, the number of time steps, the day on which the model starts, grid, initial conditions files, file with the boundary conditions, forcing parameters files with information on wind, rain, air, cloud, among others. Close the ocean_concorde.in file and start the modeling using the "bsub" function as detailed in the following figure. The modeling process took approximately 1 hour; however, this time may be longer or shorter depending on the size of the file to be modeled; in this case, it was modeled for 16 days. Therefore, the modeling time was not too long. In the end, COAWST gave us a folder with the modeled data.

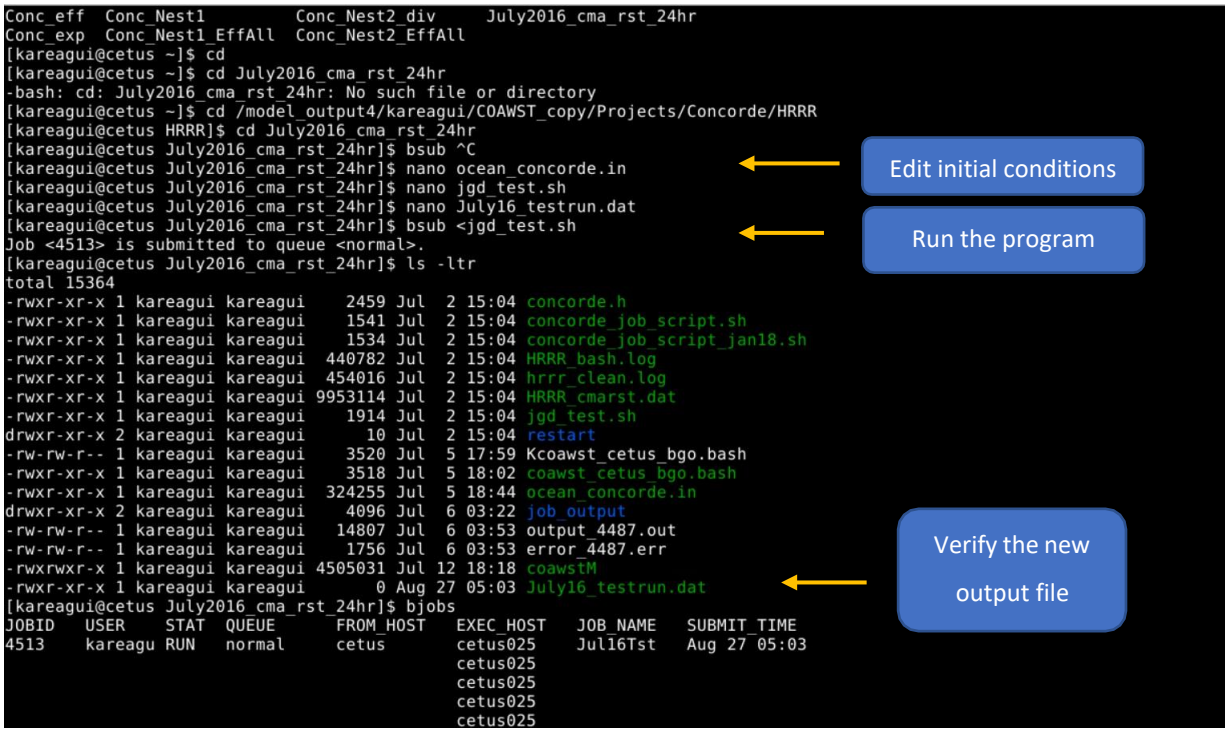

Figure 2.7 End of COAWST configuration

2.3.1 Data extraction for graphs creation

The creation of graphics and animations was done by generating a script in MATLAB. This script was modified to graph the COAWST model results of runs forced by the complete resolution wind data and the filtered wind data.

Wind timeline images were generated for each inlet. Hovmoller diagrams with red and blue color spectrum were generated to achieve greater visibility in the differences between the output of the two model runs being analyzed. Moreover, the standard deviation and mean were obtained and graphed for the surface stress of the wind, the Land Breeze Circulation (LBC), and Sea Breeze Circulation (SBC). The surface temperature and salinity of the entire study area and salinity in the water column were examined for each inlet between islands. The maximum depth considered for the generation of graphs was up to 8 meters.

Sea Breeze circulation is a very important mesoscale phenomenon. This breeze intervenes in the climatic conditions of the coastal region because it spreads from the ocean to the continental zone. The direction with which it reaches the coastline depends on four main aspects:

- The temperature gradient between the continent and the water
- Predominant flow of the boundary layer
- Elevation of the coastal region
- The shape of the coastline

The SBC also influences coastal geography and topography. The intensity and flow patterns of SBC can be affected by obstacles such as islands, peninsulas, coastal elevations, or breezes from rivers, lakes, or the mainland. An atmospheric factor that determines the location and orientation of the SBC is the predominant flow direction in the lower troposphere.

The LBC is the predominant stream at night and just before sunrise. The flow of LBC is considered weaker than that of SBC because the transverse temperature gradient of SBC is more notable than that associated with LBC. LBC convection can be observed with convergent flow located mainly over water. There are also scenarios where different LBC flows from, for example, the Louisiana coast and the Mississippi coast develop a grouped convection along the Land Breeze Front; this occurs in conditions where the angular configuration, the temperature gradient, and the Night- time decoupling of boundary layer flow overland from the prevailing synoptic wind allows this phenomenon to occur.(Hill et al., 2010)

The SBC maintains a typical evolution for all months. However, LBC shows monthly variations. During July and August, the LBC comes from eastern Louisiana, and in Mississippi, the LBC has a greater intensity in August compared to July. The LBC on the Mississippi coast is more potent than that on the Louisiana coast. Information is required that, during the night hours, especially between 11:00 p.m. and 7:00 a.m. CDT, there is high intensity of rainfall on the high seas off the coasts of Louisiana, Mississippi, and Alabama, while during the day at 11:00 CDT, the intensity of rainfall over the coastal region increases greatly, this means that during the night there is a predominance of LBC on the platform and during the day there is a predominance of SBC on the coasts. (Hill et al., 2010)

CHAPTER 3

3 RESULTS AND ANALYSIS

3.1 Study Area

The analysis of the study area was carried out with the QGIS tool. Figure 3.1 represents a global view of the American continent, and the inset located in the Gulf of Mexico shows our study area. This graph was made in this way to locate it geographically more easily on the map since many readers may not know the specific area.

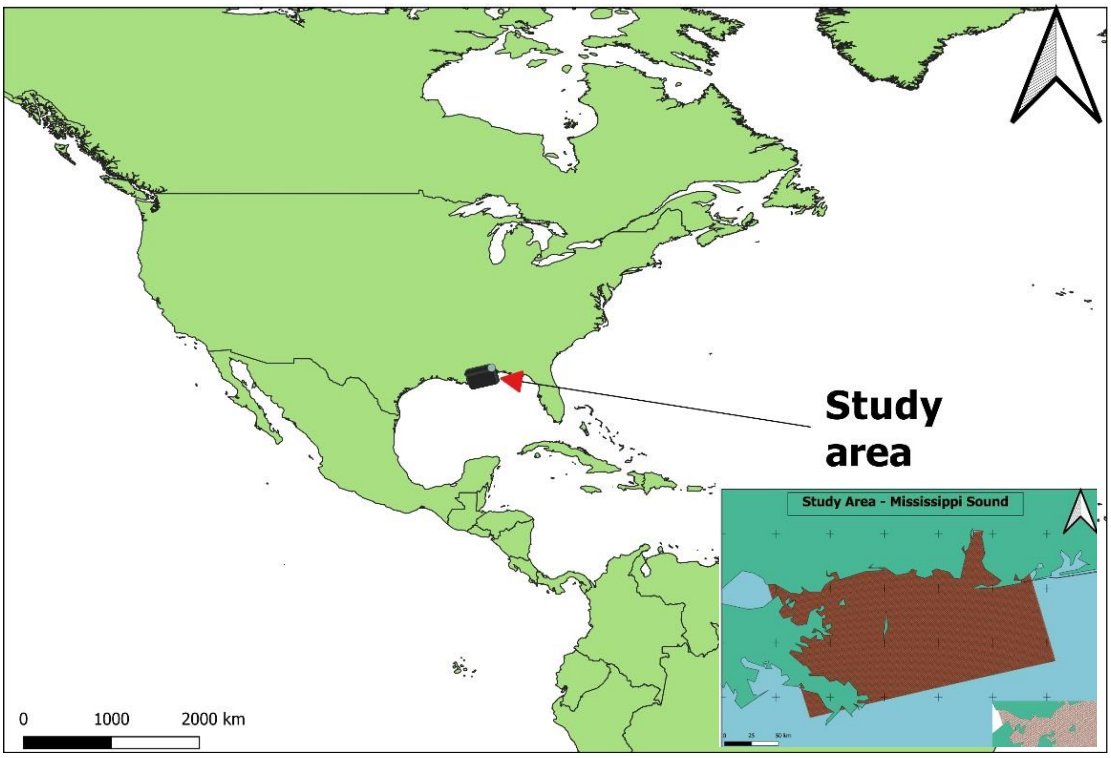

Figure 3.1 Magnified view of the study area made using QGiS

Figure 3.2 shows the study area in greater detail, consisting of 216504 points uniformly distributed within an area of 36896 km^2; it is also displayed the five islands: Cat Island, Ship Island, Horn Island, Petit Bois Island and Dauphin Island; and seven passes: Lake Pass, Cat Pass, West Ship Pass, East Ship Pass, Horn Pass, Petit Bois Pass and Main Pass.

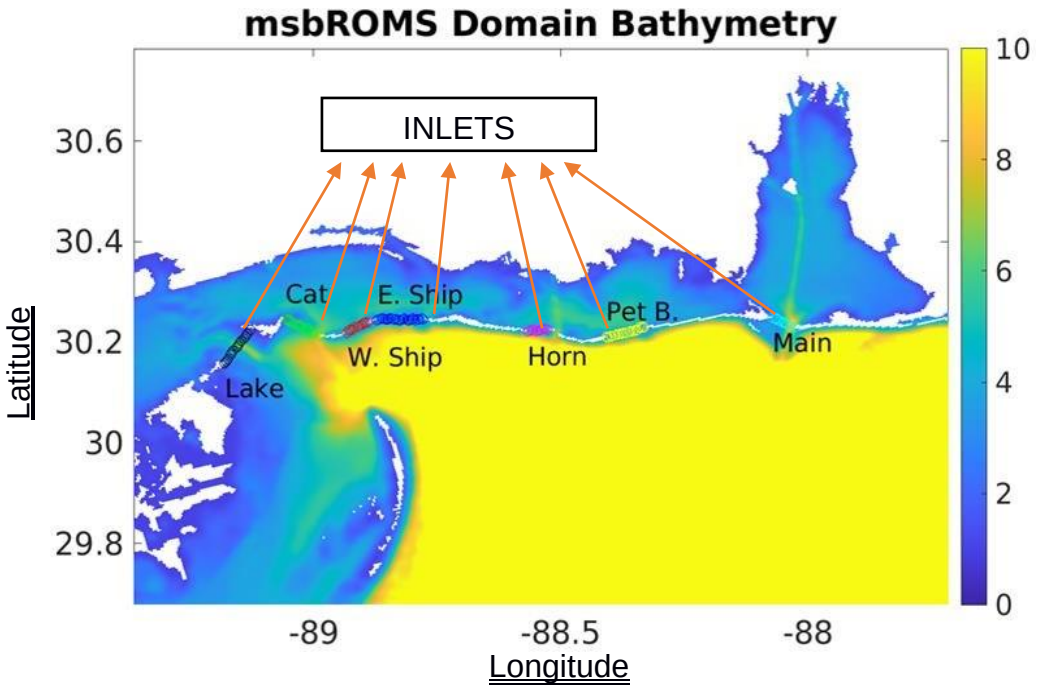

Figure 3.2 Georeferencing of the study area, barrier islands, and inlets with which we work on the project.

3.2 Wind Rose

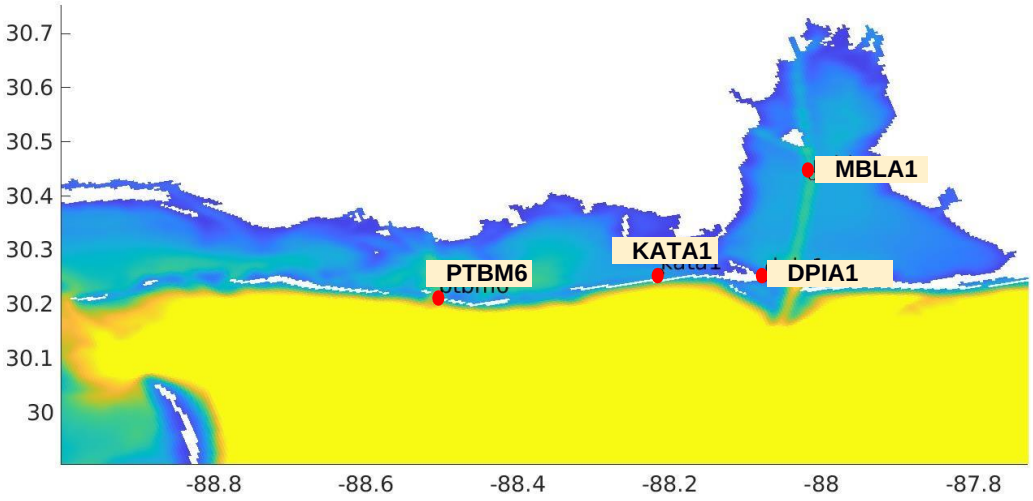

Figure 3.3 Mooring locations that were used for the generation of wind roses. Data were acquired from the National Data Buoy Center archives (NDBC).

Table 3.1 lists the wind speed and direction distribution for the HRRR (unfiltered) and HRRR24 (filtered) data sets. In general, a predominance of winds was observed

for the southern zone, which ranged between West and East. Throughout MS, there are essential gusts of winds with high values between 9 - 12 m/s; these peaks can be seen in HRRR but are absent in HRRR24. There is also considerable variation in wind speed and direction for HRRR, which is more evident in the wind coming from the north. This generalized direction towards the South was determined as a pattern of periodic events that occur each year. During June, the predominant tendency is easterly and southeasterly, and during July and August, the dominant direction is in a more notable proportion towards the South. (Hill et al., 2010)

At station DPIA1 on eastern Dauphin Island, there was a change in the wind intensity from East to West for the HRRR24 graph, with a wind speed of 7 to 9 m/s and a predominance to the Southwest. The KATA1 station at central Dauphin Island behaved similarly, while in the MBLA1 station in Mobile Bay, the wind intensity between filtered and unfiltered model solutions increased, but the direction was conserved, predominately in the Southeast and Southwest sections. As a final graph, we have the station PTBM6 on Petit Bois Island; in this location, the winds from the Southwest decreased, and they increased in the Southeast section with greater intensity.

Table 3.1 Wind Roses at NDBC's locations for HRRR unfiltered and filtered outputs

HRRR wind rose	*HRRR24 wind rose*
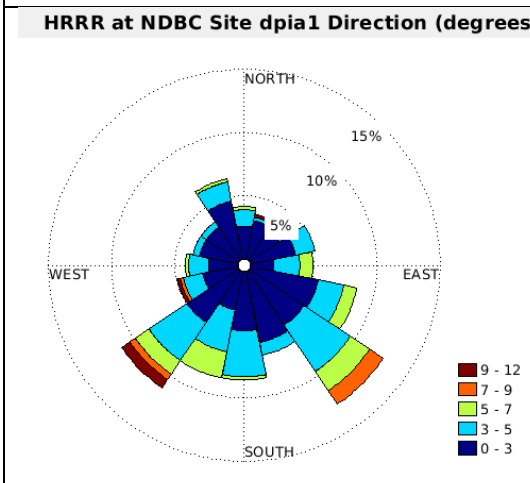	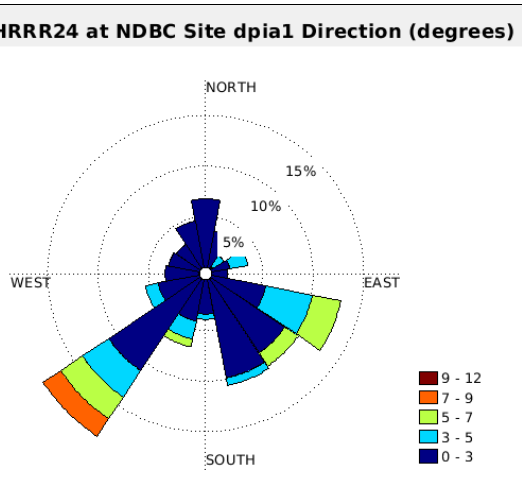

HRRR at NDBC Site kata1 Direction (degrees)

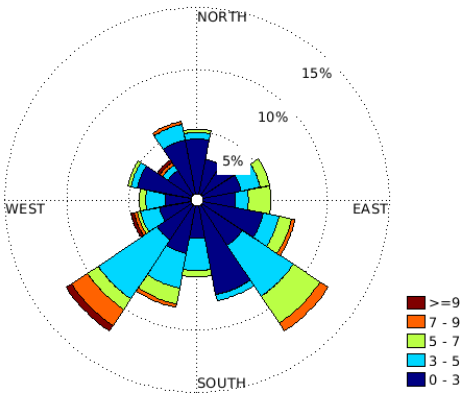

HRRR24 at NDBC Site kata1 Direction (degrees)

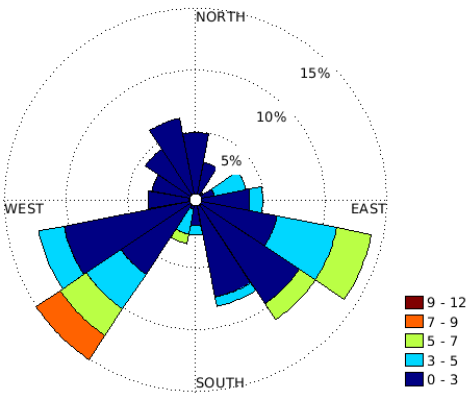

HRRR at NDBC Site mbla1 Direction (degrees)

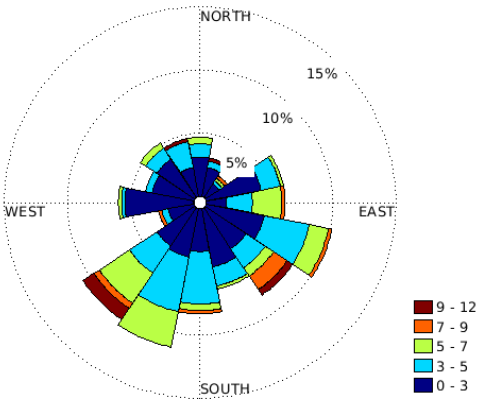

HRRR24 at NDBC Site mbla1 Direction (degrees)

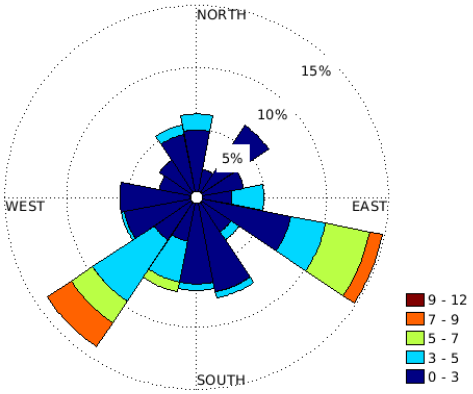

HRRR at NDBC Site ptbm6 Direction (degrees)

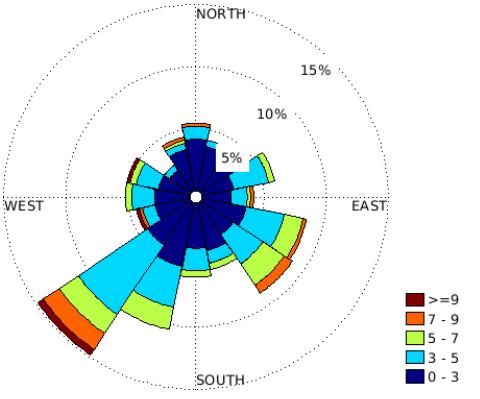

HRRR24 at NDBC Site ptbm6 Direction (degrees)

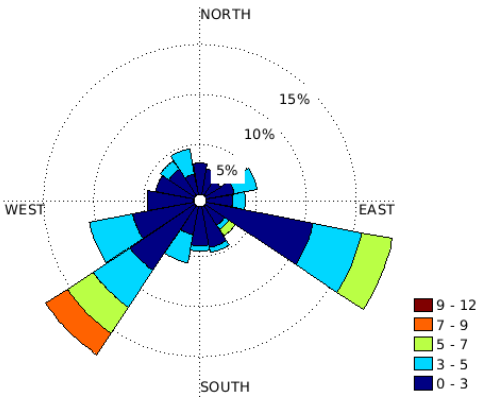

3.3 Surface Sea Temperature

During the day, two "extreme" temperature points are observed (Figure 3.4). The first is during the morning between 10 UTC and 12 UTC. During these hours, the ocean's surface temperature is low and the minimum during the day, with a value between 29 °C and 31 °C. The second point of maximum temperature occurs at night between 20 UTC and 00 UTC; during this period, the temperature fluctuates between 31°C and 33°C. These results follow the pattern of SBC and LBC mentioned above. LBC predominates in early mornings (0700-1100 CST), namely, the wind from the continental zone goes to the ocean, and this wind has a temperature higher than that of the water because the heat of the land is higher than that of the oceanic zone, therefore when entering the platform, the temperature of the surface sea increases. While at 1500-1900 CST, the shoreward SBC wind flow predominates, therefore the water temperature remains cold.

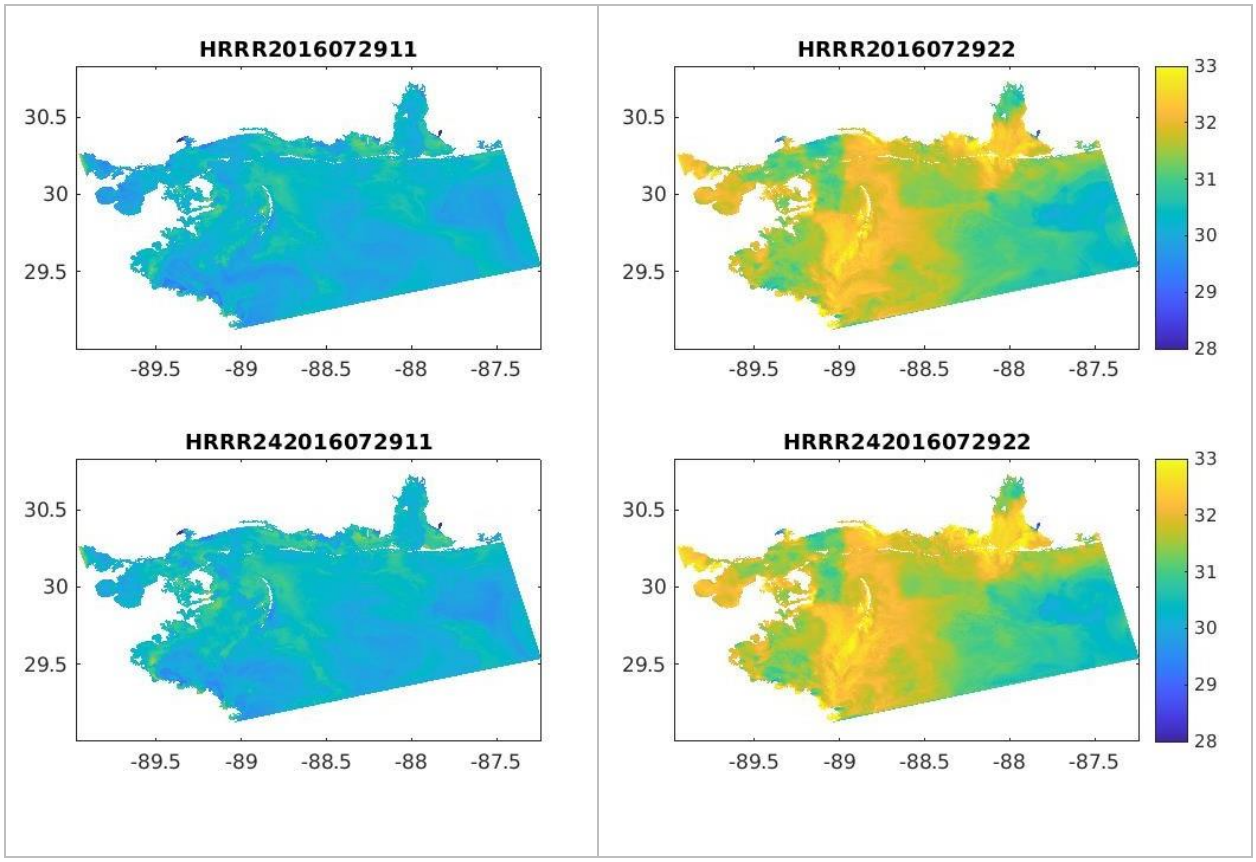

Figure 3.4 Sea Surface temperature for July 29th, 2016, at 11 UTC (left) and at 20 UTC (right)

3.4 Salinity in the water column

The salinity values are distributed expectedly in Figure 3.5, with more saline water in the deeper part and less saline in the surface water. It is essential to be clear that this body of water is fed by numerous rivers, which is why there is a distribution and mixture of fresh water and ocean water. In the standard deviation, there is a slight difference in HRRR24 to HRRR with an increase in salinity in the deep zone, while in the mean, there are no differences to document.

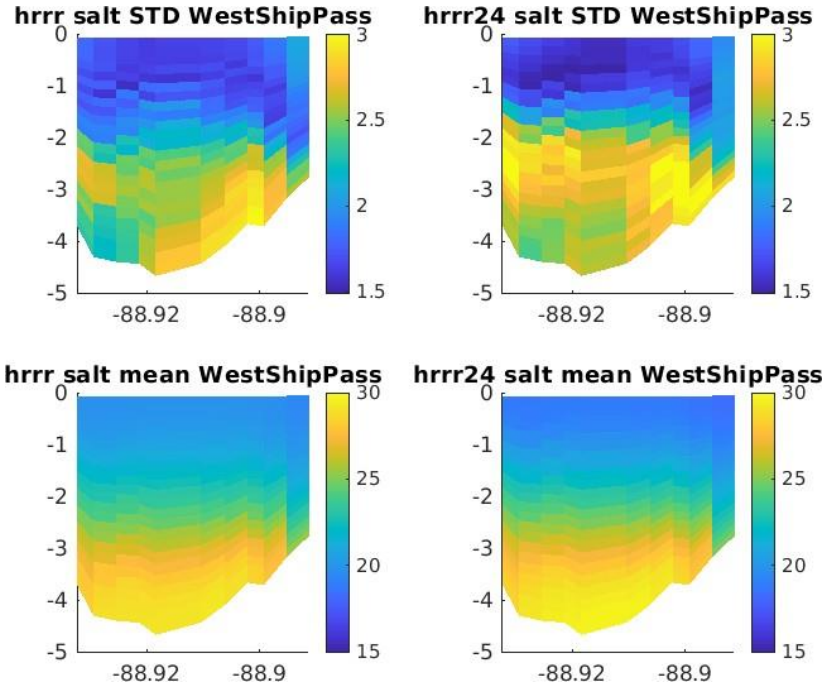

Figure 3.5 HRRR vs HRRR24 comparison for Standard deviation and Mean Salinity values in the water column in West Ship Pass

3.5 Temporal line for wind forcing data

Figure 3.6 shows the most remarkable difference results between the wind forcing filtered data and the wind forcing full-resolution data for Main Pass. In this graphic, we can distinguish a decrease by 2 m/s in the velocity of the filter data.

There was also a considerable change in the curves of Velocity vs. Time. The curves of the filtered data are much smoother and have fewer peaks. Therefore, it follows that the lowpass function did its job of interpolating and filtering out high-frequency signals such as land and sea breeze circulation.

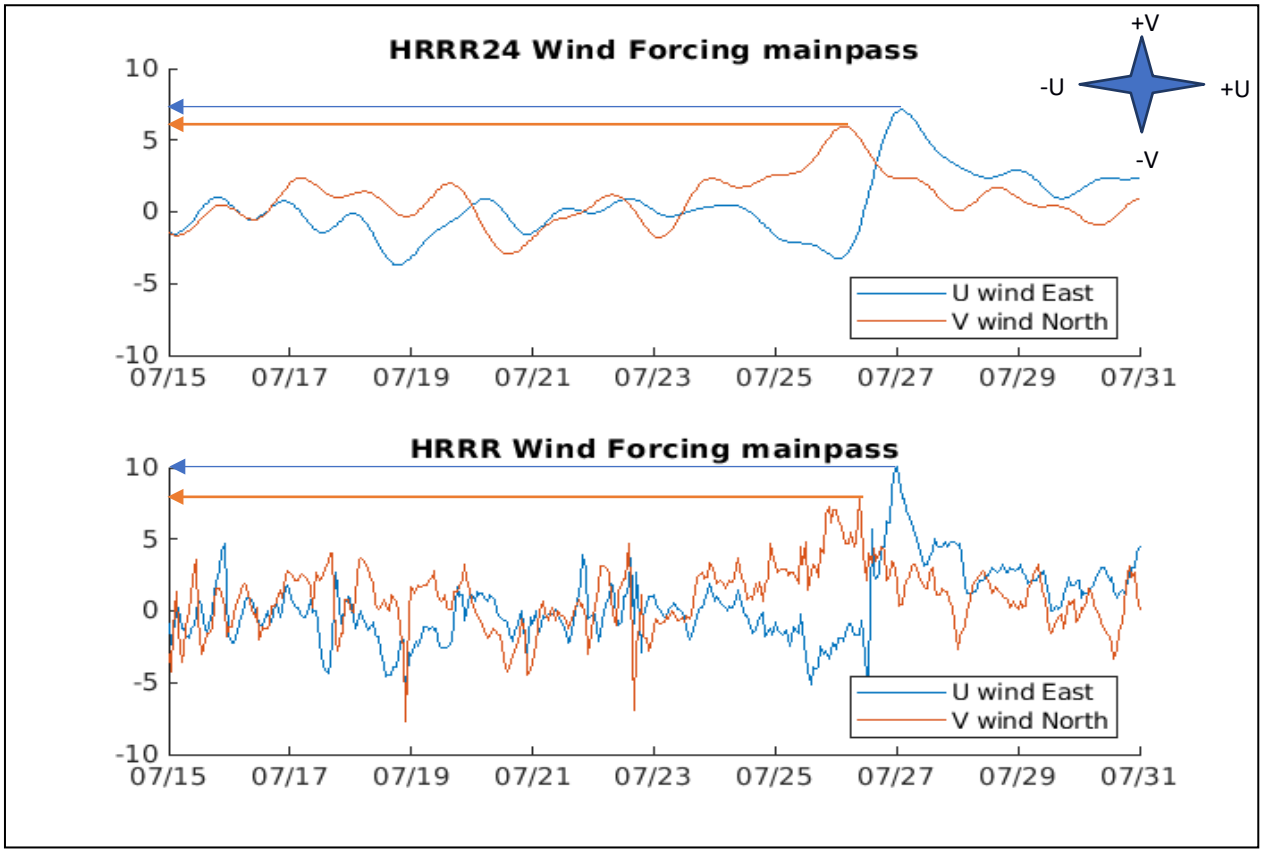

Figure 3.6 Wind filter data Vs Wind Unfiltered data - Main Pass

3.6 Comparative standard deviation Hovmoller Plots

Figures 3.7 and 3.8 show the wind velocity for vector v on the left and u on the right. In the central part are the current speeds represented in Hovmoller diagrams, in Figure 3.7 is the v current velocities or meridional velocities, and in Figure 3.8 is u current rate or zonal velocities.

The most notable differences between low-pass filtered current velocities and full-resolution current velocity are located during the low-pressure system. These differences were observed during the final days of the experiment, that is, between July 24 and 27. There are more defined reversals of the current direction in the model results forced with unfiltered wind data.

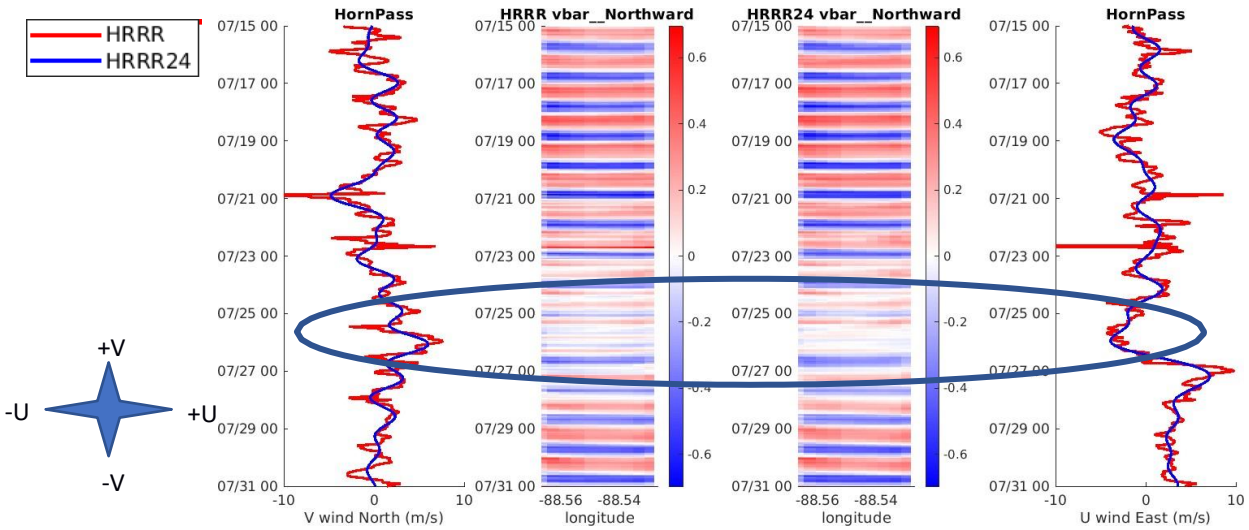

Figure 3.7 Comparison for "v" current velocity between filter and unfiltered data for Horn Island Pass

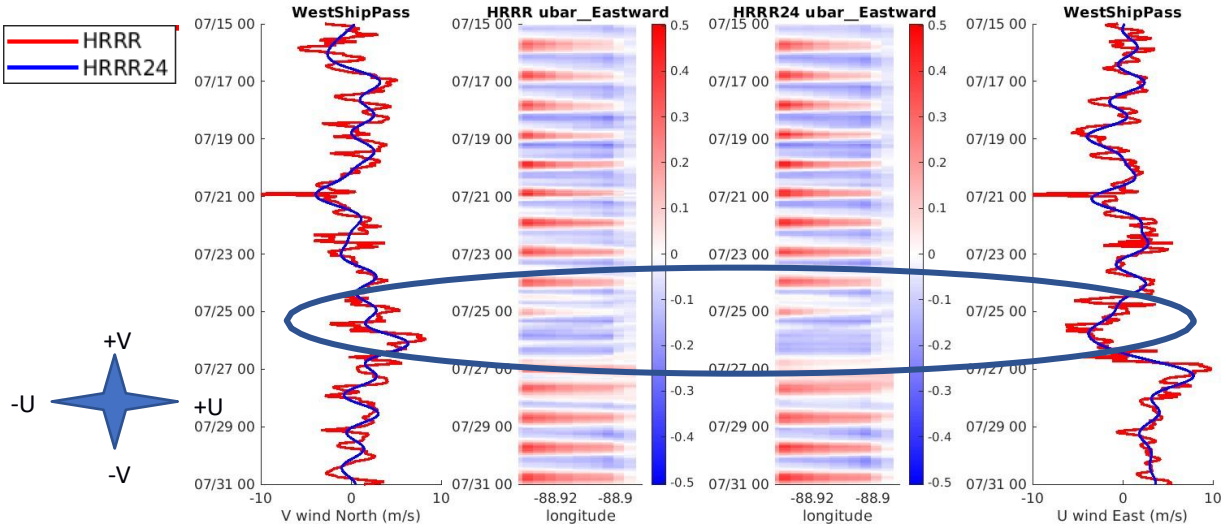

Figure 3.8 Comparison for "u" current velocity between filter and unfiltered data for Horn Island Pass

3.7 Standard deviation for u and v winds forcing vectors

In the interpretation of the standard deviation (Figure 3.9), there is a more notable difference at the Surface area (from 0 to 2 meters depth) when isolating the ocean response to LBC. The LBC wind force in Figure 3.8 Comparison for "u" current velocity between filter and unfiltered data for Horn Island Passis higher for HRRR24, especially for the surface at the longitude of -89.15, with an increase of 0.1 m/s. In SBC, the HRRR24 values show a decrease, having the highest wind force in the HRRR results throughout the entire water column.

In the full-resolution model results u eastward velocity during SBC shows a much higher standard deviation than during LBC, while in the filtered model results the current response to LBC and SBC is more consistent. This is an indication that when the high-frequency signal is filtered out variability in the current through the inlet is happening at different times during the day than with full resolution wind.

In this specific case, it can be determined that the SBC directs the circulation since it has a more critical predominance than LBC. Therefore, the convections are carried out in a north direction towards the coast. For more examples of this behavior please see Appendix B.

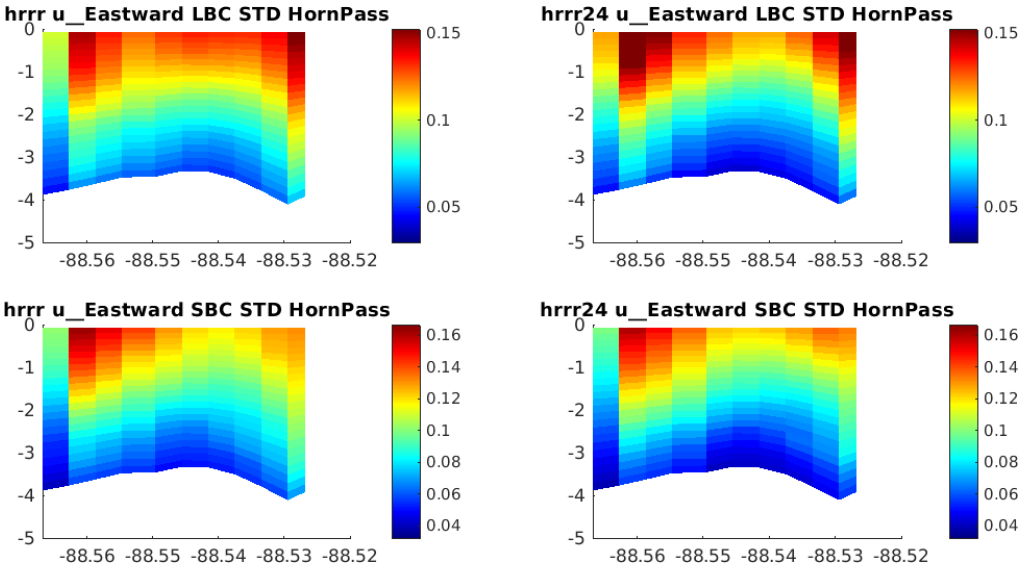

Figure 3.9 Standard deviation of u current velocity vectors for the entire two weeks in Horn Pass only for Land Breeze and Sea Breeze Circulation periods

Figure 3.10 contains the standard deviation of current velocity in the v (north) direction for the inlet between Cat Island and Ship Island. The standard deviation shows a slight increase in the current velocity variability in the N-S direction for the model output when forced with the filtered wind forcing. The lower graphs are shown values close to zero; this occurs because the force of the wind has a very similar intensity for all its directions. Therefore, when obtaining the average, the values of the graph oscillate between 0 and 0.04. The difference between HRRR and HRRR24 remains minimal, with a slight increase in wind force from HRRR24.

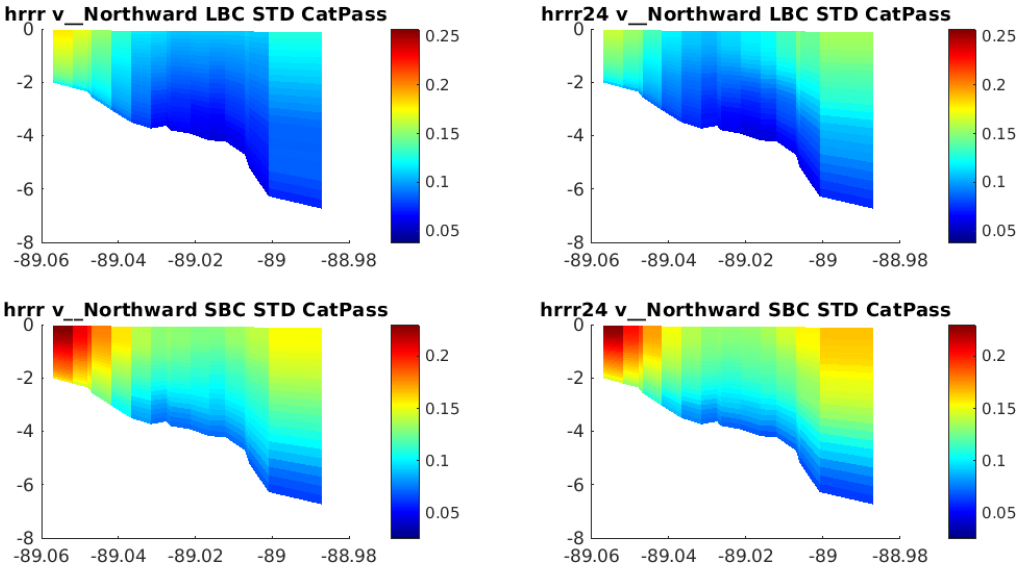

Figure 3.10 Standard deviation for v (northward) current velocity in the water column - Cat Pass over the entire 2-week only for Land Breeze and Sea Breeze Circulation periods period.

3.8 Curl Wind – Hourly range

In Figure 3.11, top of the four-time lines of wind speed (m/s) vs. time, solid lines represent HRRR24, and dotted lines represent HRRR (full-resolution data). This time series was obtained for the 16 days of data that we modeled. The two images in the lower left part show us the v (northward) current speed in the vertical cross-section of Cat Pass; in the HRRR graph, the current velocity is directed southwards (blue) on the surface and northwards (red) near the bottom and in the shallow western part of the channel. In contrast, in the filtered wind graph, it was observed that the wind has a southward direction in most of the water columns (Figures 3.11 and 3.12).

In the lower right corner are two graphs of surface wind magnitude and direction. The wind of the HRRR graph is heading south, and in the HRRR24 graph, the wind has a lower magnitude, and its direction is towards the north.

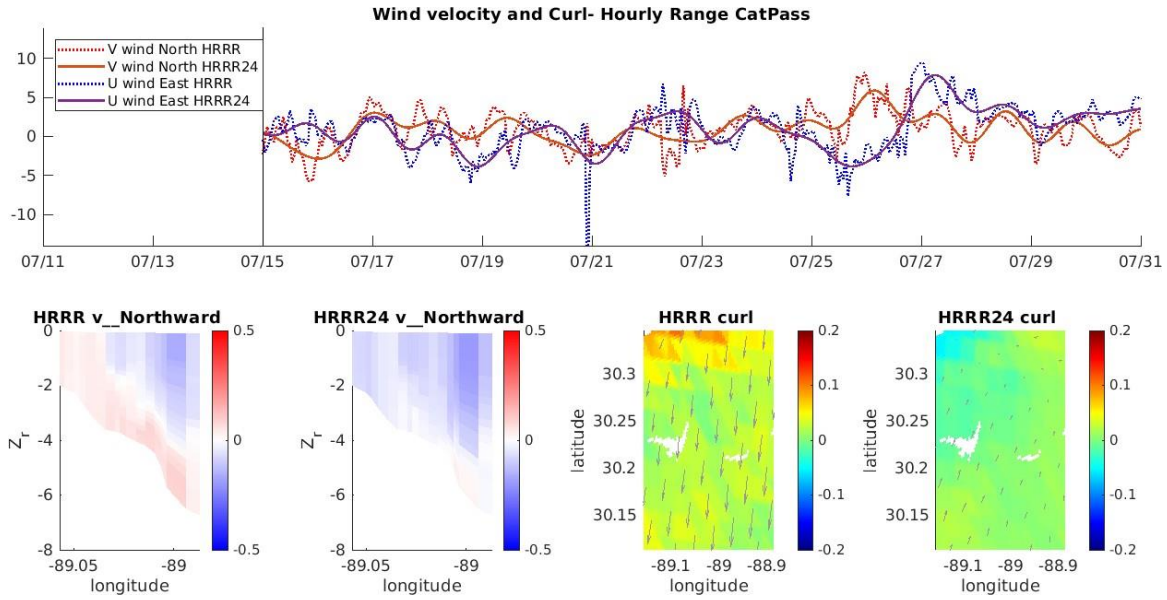

Figure 3.11 Wind and v (northward) current velocity circulation for Cat Pass on July 15, 2016, at 00:00 UTC.

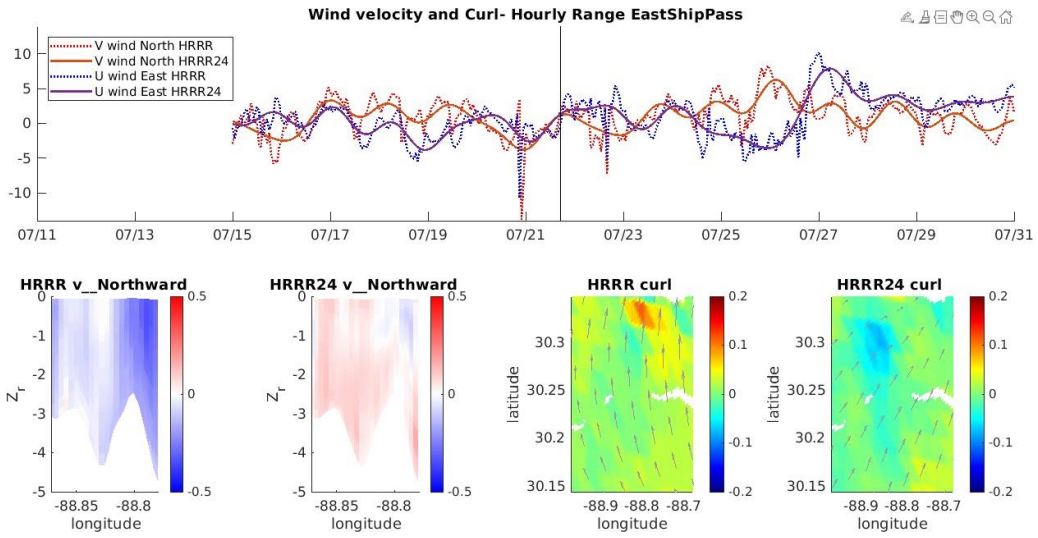

Figure 3.12 example two of Wind and v (northward) current velocity circulation for East Ship Pass on July 21, 2016, at 17:00 UTC.

3.9 Sea Breeze Circulation vs Land Breeze Circulation – Daily average

We used a daily average value for Figure 3.13, and the plots in the second row are from July 16. In the upper section, we have the same timeline as in the previous section. However, the lower graphs reflect different variables: the two lower graphs on the left correspond to Land Breeze Circulation; for this variable, a slight increase in

HRRR24 was observed with a northward direction for both graphs. The two lower graphs on the right represent Sea Breeze Circulation with a substantial increase and change of direction in HRRR24, involving, in the HRRR results was observed a direction slightly to the north on the surface and slightly to the south in the deep zone with an inclination present from the surface. At the same time, in HRRR24, the entire water column has a more intense breeze directed towards the north.

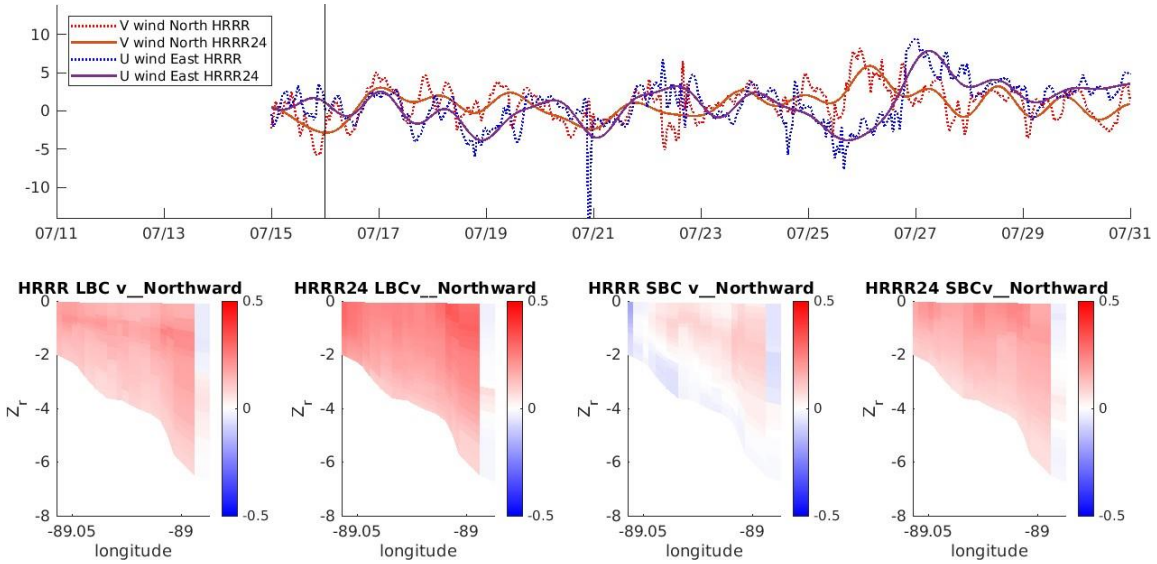

Figure 3.13 Sea and Breeze circulation snapshot for Cat Pass: 07/16/2016 at 1100 UTC

3.10 Costs Analysis

This project englobes different software and tools that, the same ones that will be listed in Table 3.2:

Table 3.2 Cost analysis

Software/Tool	Cost	Observations
MATLAB	*ESPOL - License N°: 365148*	Depends on the type of industry that you are working for.
COAWST	Open source (free)	(John Warner et al., 2010)
Data collector	Open source (free)	(Blaylock et al., 2018)
QGiS	Open source (free)	(QGIS.org, 2021)

CHAPTER 4

4. CONCLUSIONS AND RECOMMENDATIONS

4.1 Conclusions

- The algorithm development to filter and interpolate the wind forcing file was successful. The peaks or extreme values as high frequency were ignored, and only those recurring values were conserved, creating a smooth temporal line of wind velocity.

- The result obtained with the filter was similar to that obtained with NARR; however, it cannot be said that the filtered results are 100% equal to those of the NARR product since they are obtained under different conditions, and the modeling process is not the same. Therefore, it could not give an identical product but is similar enough to be representative. To obtain a result capable of being 100% equivalent to NARR, the code would have to be modified by coupling the filter, the data, and the boundary conditions to the parameters and requirements used by the NARR product.

- The models obtained through COAWST met the expectations showing all the variables needed to create the graphics and make the required comparisons.

- The differences between the full resolution wind force modeling and the filtered wind force file are based on the data entered in the COAWST model. Namely, the model did not change the results but modeled the files inputs from the two data sets, where the first data set (full resolution) was composed of all wind speeds such as wind gusts, high-speed peaks, low-speed peaks, among others. While the other set of data (filtered) only had almost constant wind values. The other variables such as temperature, salinity, cloudiness, rain, and others. They were not filtered or modified; therefore, both models had the same additional variables as a basis to complement and obtain results closer to reality.

- The comparison between both sets of wind force showed a notable difference in resolution, showing that HRRR has a high resolution since it manages to capture specific scenarios of gusts of wind, temperature, and salinity that the HRRR24 model (filtered file) failed to capture due to its low data resolution.

- The areas with the greatest vulnerability to sudden changes in winds, and the oceanic behavior in front of these events, were determined, which are found mostly within the inlets between barrier islands and in the shallow depths of the Mississippi Sound.

- The inlets are the most vulnerable areas because they do not have coastal fronts to protect them, which causes the wind to enter strongly through them. In addition, part of the wind that hits the islands is due to the inlets and enters through them, therefore, has a high incidence of wind uptake and transit. On the other hand, the body of water located between the coast and the MS is shallow, which increases its vulnerability and risk to meteorological factors. This does not happen on the same scale in the high seas since the depth and area characteristics work as a method of protection against meteorological events.

- The HRRR high-resolution product was verified to be the best available for the Mississippi area. Therefore, this product will be used in future projects to research and understand the complex dynamics of the study area.

4.2 Recommendations

- It is recommended to carry out the model comparison experiment for a longer period to obtain more precise and accurate results.

- Because this project was carried out for 16 days, there could be different or more precise results regarding the comparisons between both models if the same analysis were taken, but for example, for a period of one year, since in that scenario would take all the seasons of the year and the changes that occur during each of them. However, we cannot assure that there are differences as it has not been tried before.

- For future work, it is advisable to replicate the experiment in another area to verify the versatility of the project against different scenarios. To replicate the work, we would only need global wind data taken from any instrument; however, these data should meet specific requirements such as having hourly temporal resolution and must also be adapted to the HRRR product to be able to model them in COAWST and obtain the expected results.

- Compare the results of the HRRR model with real files taken on-site to verify the high precision and accuracy of the model. Replicate this exercise with data from extreme events such as hurricanes and storms and compare the outputs obtained with the accidents caused in the study area.

- Include more high-resolution products available in the industry to find more accurate modeling.

BIBLIOGRAPHY

Armstrong B. N., D. Bernstein, S. Kalathupurath Kuttan, M.K. Cambazoglu, & J.D. Wiggert. (2021). Wind Sensitivity Analysis in a COAWST Model of the Mississippi Sound. *School of Ocean Science & Engineering Marine Science Division, Stennis Space Center, MS*.

Blaylock, B. K., Horel, J. D., & Galli, C. (2018). High-Resolution Rapid Refresh Model Data Analytics Derived on the Open Science Grid to Assist Wildland Fire Weather Assessment. *Journal of Atmospheric and Oceanic Technology*, *35*(11), 2213–2227. https://doi.org/10.1175/JTECH-D-18-0073.1

Blaylock, B. K., Horel, J. D., & Liston, S. T. (2017). Cloud archiving and data mining of High-Resolution Rapid Refresh forecast model output. *Computers & Geosciences*, *109*, 43–50. https://doi.org/10.1016/j.cageo.2017.08.005

Boulder, C. U. (2020, June 3). *Unidata | NetCDF*. https://www.unidata.ucar.edu/software/netcdf/

Curray, J. R., & Moore, D. G. (1963). *Facies delineation by acoustic reflection: Sedimentology*. *2*, 130–148.

Dougherty, K. J. (2020). *EVALUATION OF THE HIGH-RESOLUTION RAPID REFRESH AND THE COUPLED OCEAN-ATMOSPHERE MESOSCALE PREDICTION SYSTEM DURING ATMOSOPHERIC RIVER EVENTS IN CALIFORNIA*.

FEMA. (2006). High water mark collection for hurricane Katrina in Luisiana. *Federal Emergency Management Agency*, 412–419.

Fritz, H. M., Blount, C., Sokoloski, R., Singleton, J., Fuggle, A., McAdoo, B. G., Moore, A., Grass, C., & Tate, B. (2007). Hurricane Katrina storm surge distribution and field observations on the Mississippi Barrier Islands. *Estuarine, Coastal and Shelf Science*, *74*(1–2), 12–20. https://doi.org/10.1016/j.ecss.2007.03.015

Gowan, T. A. (2021). *DATA ANALYTICS APPLIED TO SATELLITE-DERIVED PRECIPITATION ESTIMATES AND HIGH-RESOLUTION MODEL OUTPUT*.

Greer, A., Shiller, A., Hofmann, E., Wiggert, J., Warner, S., Parra, S., Pan, C., Book, J., Joung, D., Dykstra, S., Krause, J., Dzwonkowski, B., Soto, I., Cambazoglu, K., Deary, A., Briseño-Avena, C., Boyette, A., Kastler, J., Sanial, V., … Graham, W.

(2018). Functioning of Coastal River-Dominated Ecosystems and Implications for Oil Spill Response: From Observations to Mechanisms and Models. *Oceanography*, *31*(3). https://doi.org/10.5670/oceanog.2018.302

Hill, C. M., Fitzpatrick, P. J., Corbin, J. H., Lau, Y. H., & Bhate, S. K. (2010). Summertime precipitation regimes associated with the Sea Breeze and Land Breeze in Southern mississippi and Eastern Louisiana. *Weather and Forecasting*, *25*(6), 1755–1779. https://doi.org/10.1175/2010WAF2222340.1

Hossain, N. U. I., Nur, F., Hosseini, S., Jaradat, R., Marufuzzaman, M., & Puryear, S. M. (2019). A Bayesian network based approach for modeling and assessing resilience: A case study of a full service deep water port. *Reliability Engineering & System Safety*, *189*, 378–396. https://doi.org/10.1016/J.RESS.2019.04.037

Hwang, P. A., Teague, W. J., Jacobs, G. A., & Wang, D. W. (1998). A statistical comparison of wind speed, wave height, and wave period derived from satellite altimeters and ocean buoys in the Gulf of Mexico region. *Journal of Geophysical Research: Oceans*, *103*(C5), 10451–10468. https://doi.org/10.1029/98JC00197

Iowa State University. (2021). *Iowa Environmental Mesonet :: Custom Wind Roses*. https://mesonet.agron.iastate.edu/sites/dyn_windrose.phtml?station=BIX&network=MS_ASOS&bin0=2&bin1=5&bin2=7&bin3=10&bin4=15&bin5=20&units=mps&nsector=36&fmt=png&dpi=100&year1=2016&month1=1&day1=1&hour1=0&minute1=0&year2=2016&month2=12&day2=1&hour2=23&minute2=0

Kantha L., Choi J. K., Leben R., Cooper C., Chevron, Vogel M., & Feeney J. (1999). Hindcasts and Real-time Nowcast/Forecasts of Currents in the Gulf of Mexico. *Offshore Technology Conference*.

Knabb, R. D., Rhome, J. R., & Brown, D. P. (2005). *Tropical Cyclone Report Hurricane Katrina.* .

Moncreiff Cynthia A., Handley L., & Altsman D. (2007). *Seagrass Status and Trends in the Northern Gulf of Mexico: 1940–2002*. USGS. https://pubs.usgs.gov/sir/2006/5287/pdf/CoverandContents.pdf

Morton, R. A. (2003). *An overview of coastal land loss: with emphasis on the southeastern United States: U.S. Geological Survey Open-file Report 03-337, 28p*.

Morton Robert A. (2007). Historical Changes in the Mississippi-Alabama Barrier Islands and The Roles Of Extreme Storms, Sea Level and Human Activities. In *US Geological Survey - Science for a changing world*. https://pubs.usgs.gov/of/2007/1161/OFR-2007-1161-screen.pdf

Nelson, D. (2015). *Estuarine Salinity Zones In Gulf of Mexico Atlas [Internet]*. Stennis Space Center (MS): National Centers for Environmental Information. https://www.ncei.noaa.gov/maps/gulf-data-atlas/atlas.htm

NOAA. (2021). *NOAA Tides and Currents*. https://tidesandcurrents.noaa.gov/

Sanibel Sea School. (n.d.). *Currents in the Gulf of Mexico | The Coastal Classroom*. Retrieved September 6, 2021, from http://classroom.sanibelseaschool.org/currents-in-the-gulf-of-mexico

Schmid K. (2000). Historical evolution of Mississippi's barrier Islands. *Mississippi Enviroment*.

Seidov, D., Mishonov, A. v, Boyer, T. P., Baranova, O. K., Nyadjro, E., Arthur R, & Weathers, K. A. (2020). *Gulf of Mexico Regional Climatology version 2 (NCEI Accession 0222571)*. NOAA National Centers for Environmental Information. https://www.ncei.noaa.gov/access/metadata/landing-page/bin/iso?id=gov.noaa.nodc:0222571

Seim, H. E., Kjerfve, B., & Sneed, J. E. (1987). Tides of Mississippi Sound and the adjacent continental shelf. *Estuarine, Coastal and Shelf Science*, *25*(2), 143–156. https://doi.org/10.1016/0272-7714(87)90118-1

U.S. Fish and Wildlife Service. (1982). *Mississippi Sound | GulfBase*. Mississippi Sound, Gulf Coast Ecological Inventory Map. https://www.gulfbase.org/geological-feature/mississippi-sound

USACE. (1969). Hurricane Camile 14-22 August 1969. *United States Army Corps of Engineers, Mobile, Alabama*, 199.

Vitart, F., Anderson, J. L., & Stern, W. F. (1997). Simulation of Interannual Variability of Tropical Storm Frequency in an Ensemble of GCM Integrations. *Journal of Climate*, *10*(4). https://doi.org/10.1175/1520-0442(1997)010<0745:SOIVOT>2.0.CO;2

Warner John, Armstrong Brandy, & Zambon J. (2010). *Coupled-Ocean-Atmosphere-Wave-Sediment Transport (COAWST) Modeling System*. Development of a Coupled Ocean-Atmosphere-Wave-Sediment Transport (COAWST) Modeling System: Ocean Modeling. https://www.usgs.gov/software/coupled-ocean-atmosphere-wave-sediment-transport-coawst-modeling-system

APPENDIX

Appendix A

MATLAB script: wind forcing filter file

This script was created by Brandy Armstrong and modified and adapted to the situation presented in this work by Karen Aguirre

```
clc
clear all
close all
addpath(genpath('/home/kareagui/Documents/MATLAB/'))        %Add work diectory

start_date=datenum(2016,07,16,0,0,0);                       %Set project start and
                                                            end date
end_date=datenum(2016,07,31,18,0,0);

tmp_path =
'/home/panc/work/Concorde/concorde_forcing/2017_06_06_filter_forcing/mat_tmp/';
frc_file_ori =
'/concorde2/modelers/brandy_model_runs/Forcing/WIND_july15_31_2016_HRRR.nc';

frc_file_UV =
'/home/kareagui/Documents/MATLAB/WIND_july15_31_2016_HRRR_24.nc';

lon_frc = ncread(frc_file_ori,'lon');                       %Read latitude and
                                                            longitude
lat_frc = ncread(frc_file_ori,'lat');
[MM,NN] = size(lon_frc);                                    %Matrix creation
M2=lon_frc(:);
M3=lat_frc(:);
M4=[M2,M3];
writematrix(M4,"LatLong.csv");                              %Creation of file with
                                                            latitude and longitude data
                                                            for georeferencing in Qgis


tstep = 1;                                                  %Time steps
hour_filt = 24;                                             %number of hours with data
                                                            per day


Uwind = ncread(frc_file_ori,'Uwind');                       %Read the wind forcing in
                                                            both vectors
Vwind = ncread(frc_file_ori,'Vwind');
```

```
%Wind filtering:

for i = 1:MM
   i
   for j = 1:NN

      Uwind_tmp = squeeze(Uwind(i,j,:));
      Vwind_tmp = squeeze(Vwind(i,j,:));

      Uwind_filt(i,j,:) = lowpass(Uwind_tmp,1,tstep,hour_filt,tstep,2,hour_filt);
      Vwind_filt(i,j,:) = lowpass(Vwind_tmp,1,tstep,hour_filt,tstep,2,hour_filt);

   end
end
ncwrite(frc_file_UV,'Uwind',Uwind_filt);          %Creation of Nc file to
                                                  model in COAWST
ncwrite(frc_file_UV,'Vwind',Vwind_filt);
%%
figure;
plot(squeeze(Uwind_filt(1,1,:)));
hold on;
plot(squeeze(Uwind(1,1,:)));
figure;
plot(squeeze(Vwind_filt(1,1,:)));
hold on;
plot(squeeze(Vwind(1,1,:)));
```

Appendix B

Access link to all the products of this project:

https://drive.google.com/drive/folders/138G2wSGlaOAACIsri8L0HbFagWxftjl6?usp=sharing

Appendix C

Hovmoller diagrams

U vector:

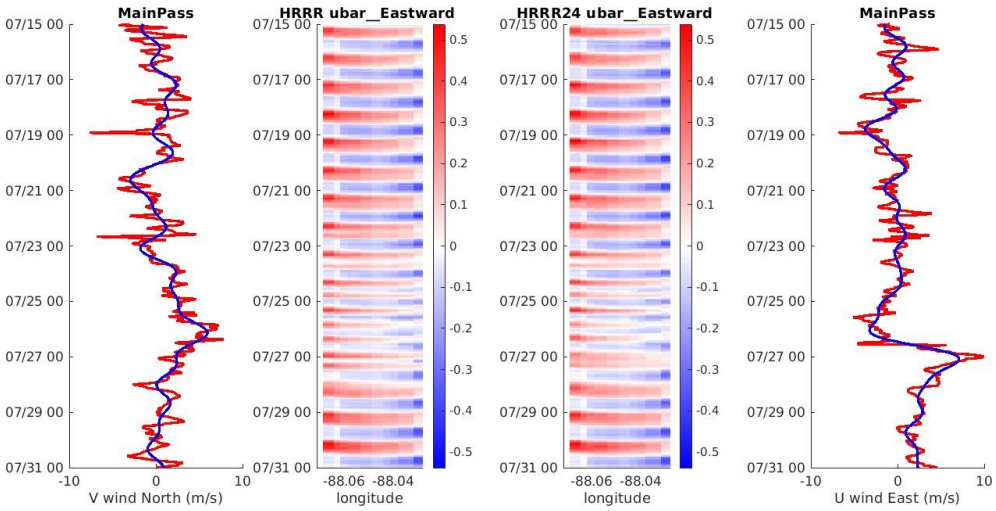

Main pass hovmoller comparison between u wind forcing HRRR vsHRRRR24

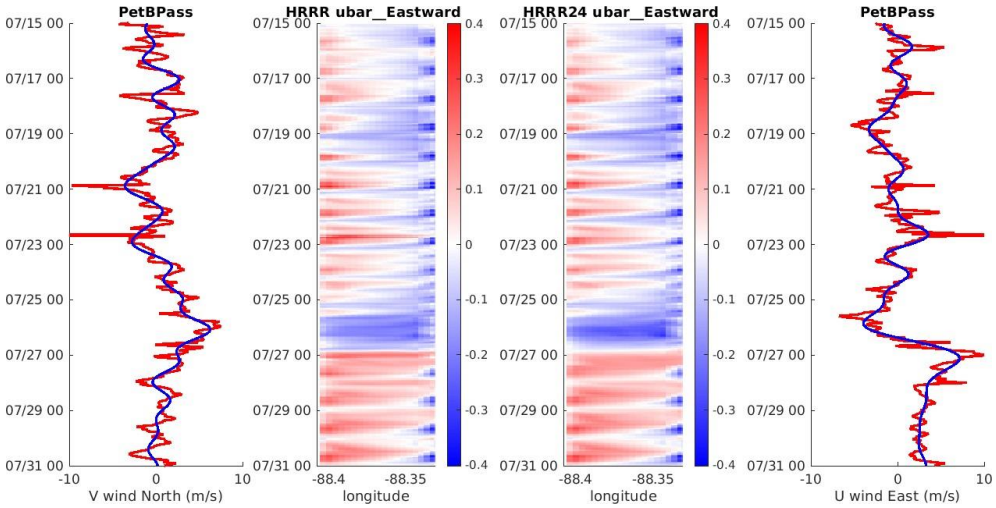

Petit Bois pass hovmoller comparison between u wind forcing HRRR vs HRRRR24

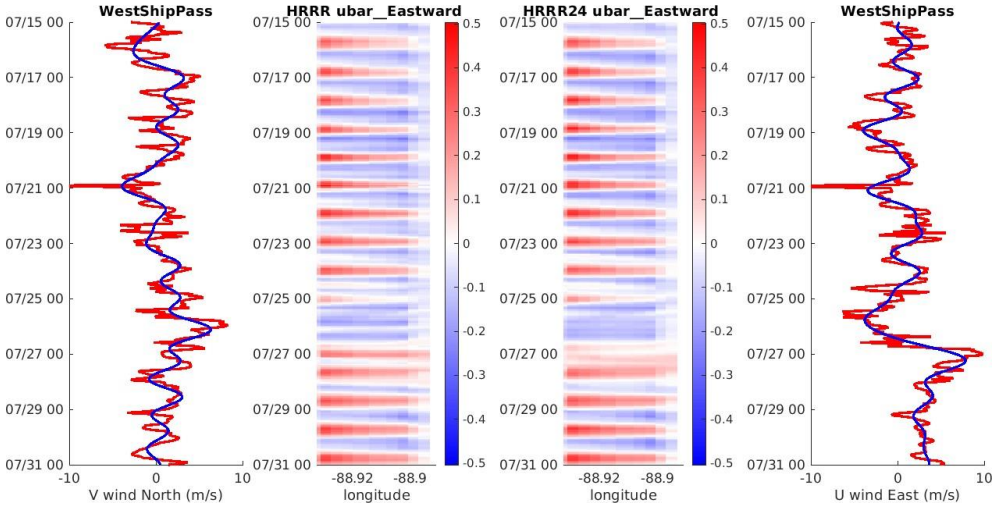

West Ship pass hovmoller comparison between u wind forcing HRRR vs HRRRR24

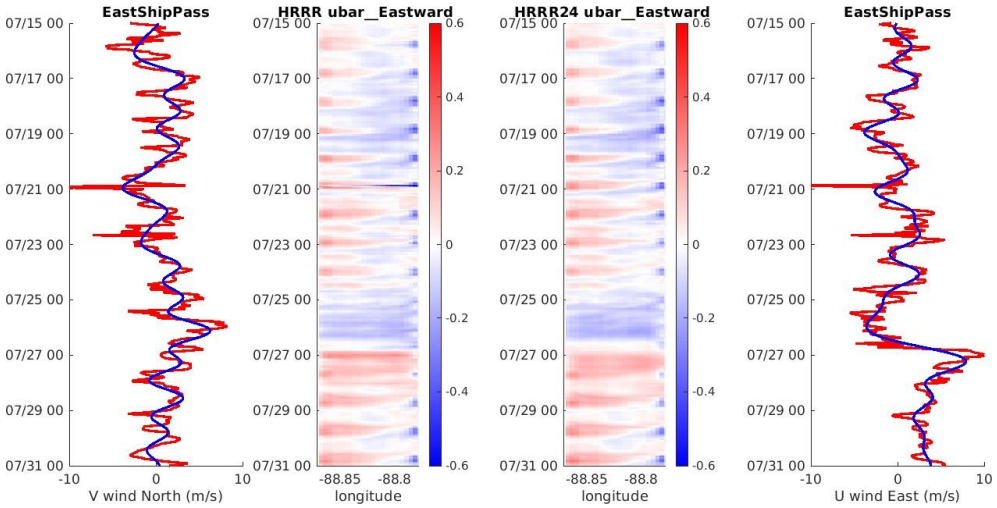

East pass hovmoller comparison between u wind forcing HRRR vs HRRRR24

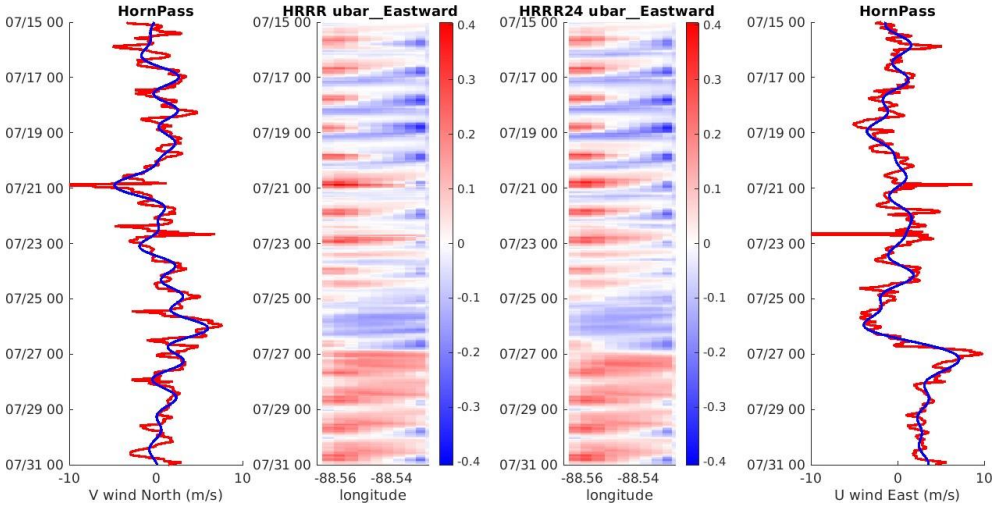

Horn pass hovmoller comparison between u wind forcing HRRR vs HRRRR24

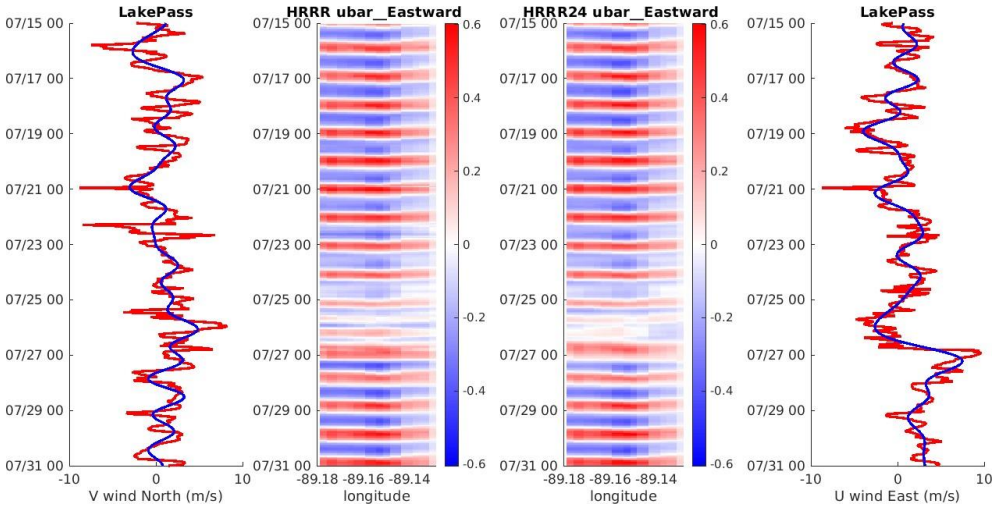

Lake pass hovmoller comparison between u wind forcing HRRR vs HRRRR24

V vector:

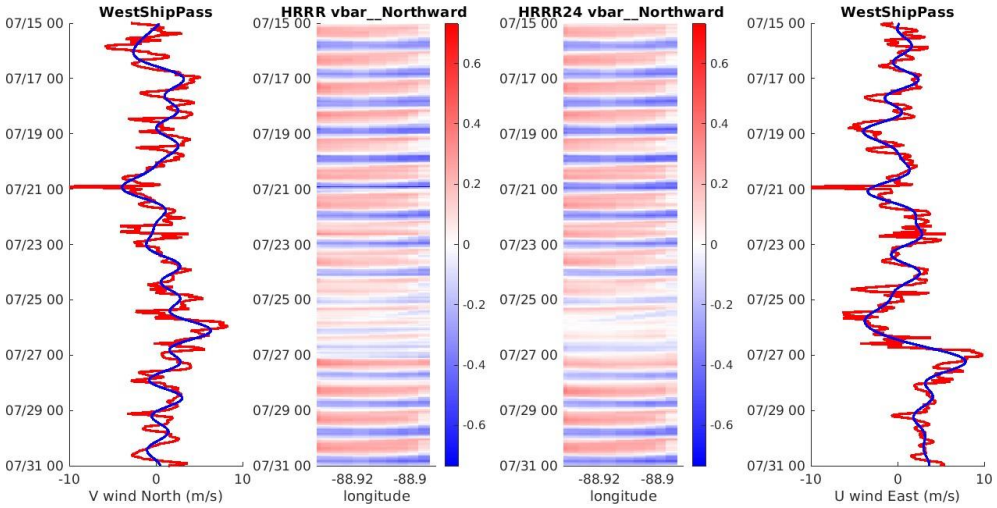

West Ship pass hovmoller comparison between v wind forcing HRRR vs HRRRR24

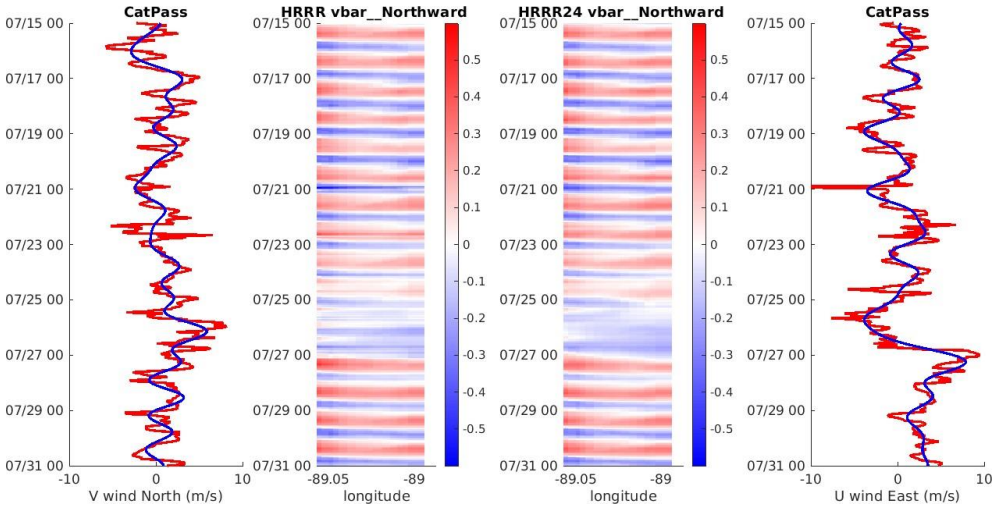

Cat Pass hovmoller comparison between v wind forcing HRRR vs HRRRR24

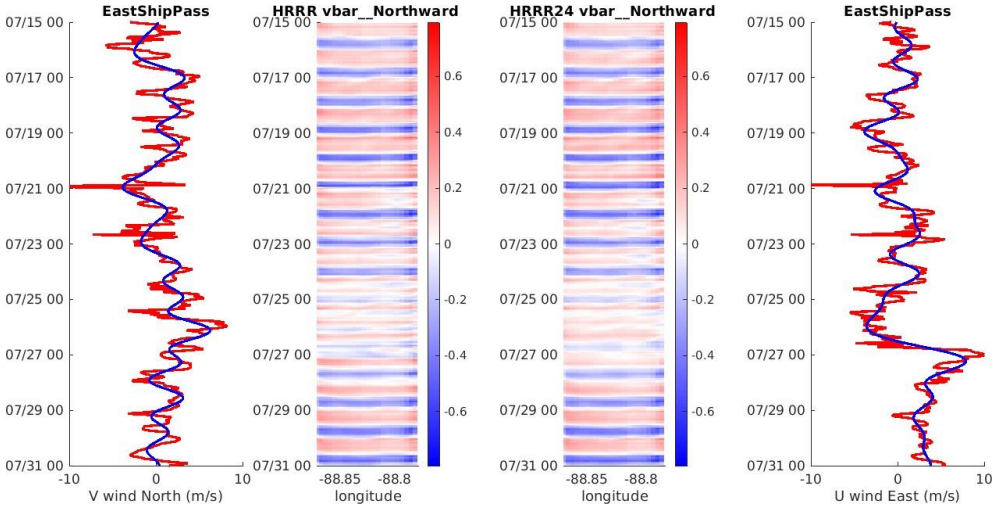

East Ship pass hovmoller comparison between v wind forcing HRRR vs HRRRR24

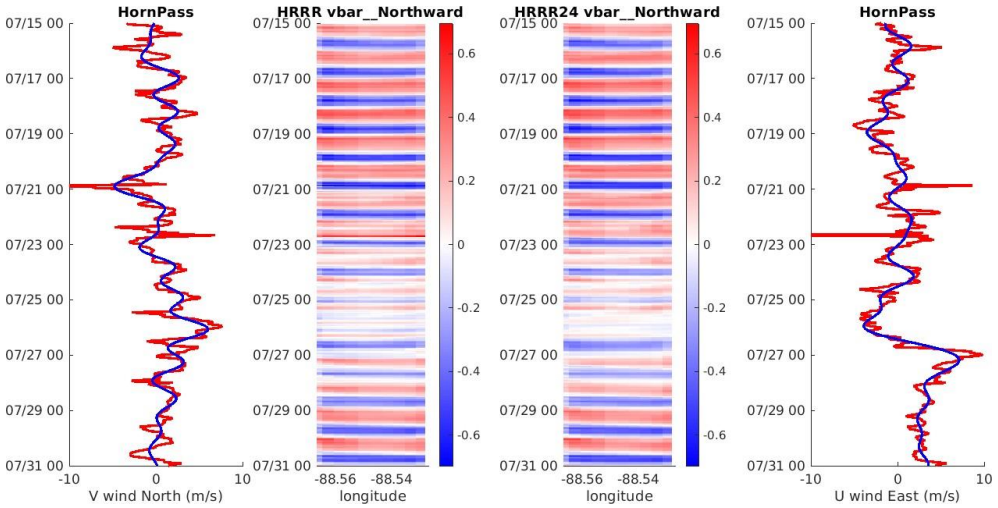

Horn pass hovmoller comparison between v wind forcing HRRR vs HRRRR24

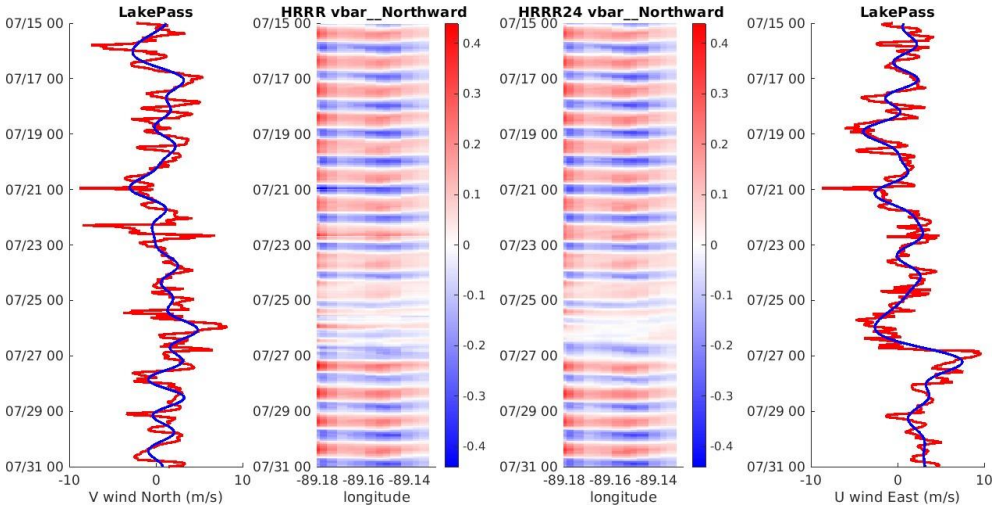

Lake pass hovmoller comparison between v wind forcing HRRR vs HRRRR24

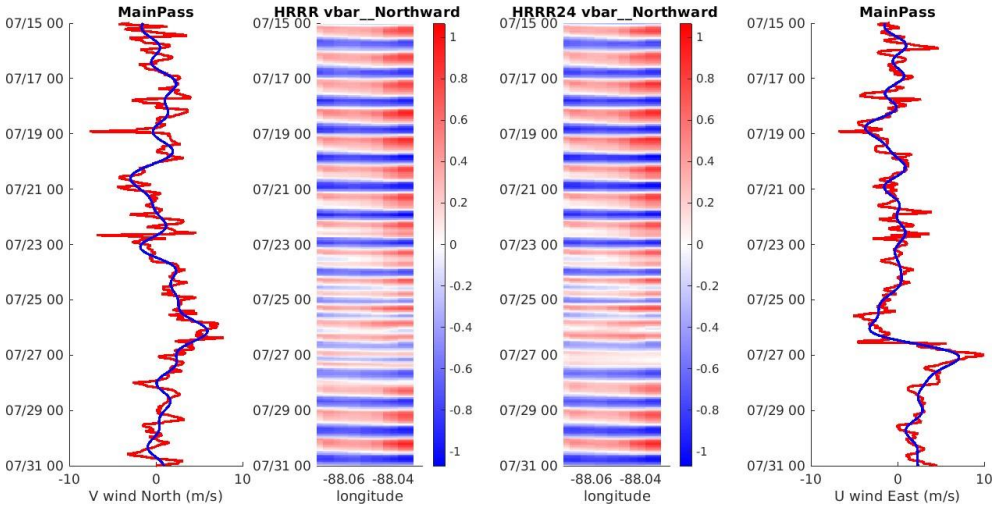

Main pass hovmoller comparison between v wind forcing HRRR vs HRRRR24

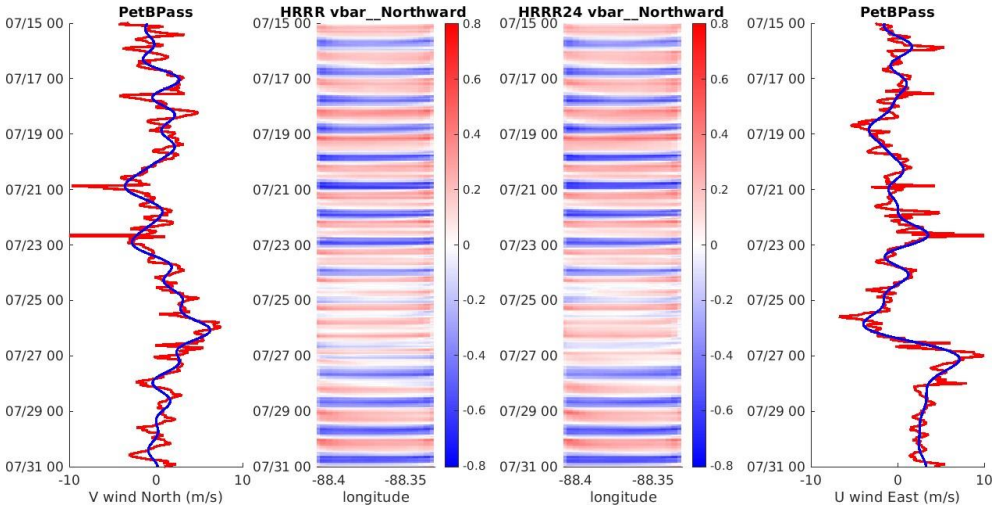

Petit Bois Pass hovmoller comparison between v wind forcing HRRR vs HRRRR24

Superficial U vector stress:

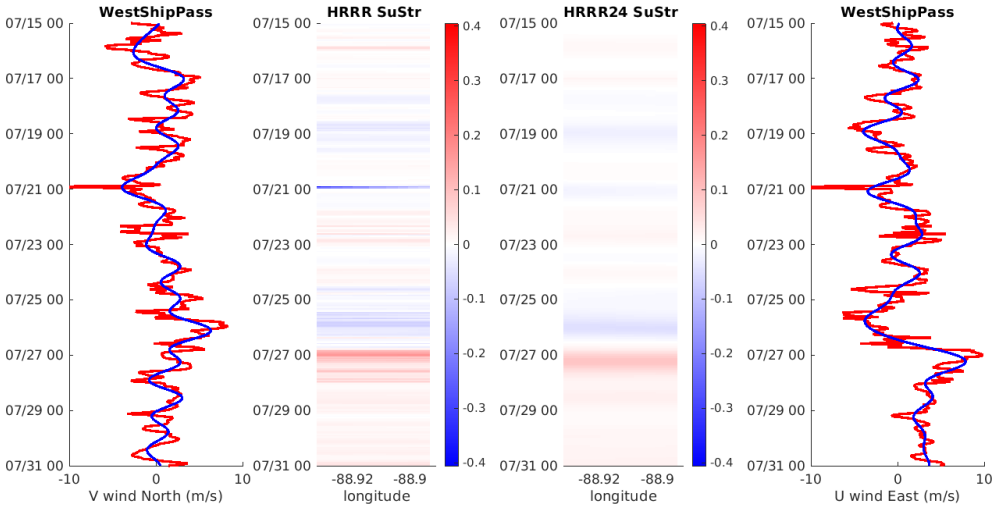

West Ship pass Superficial stress comparison between u wind forcing HRRR vs HRRRR24

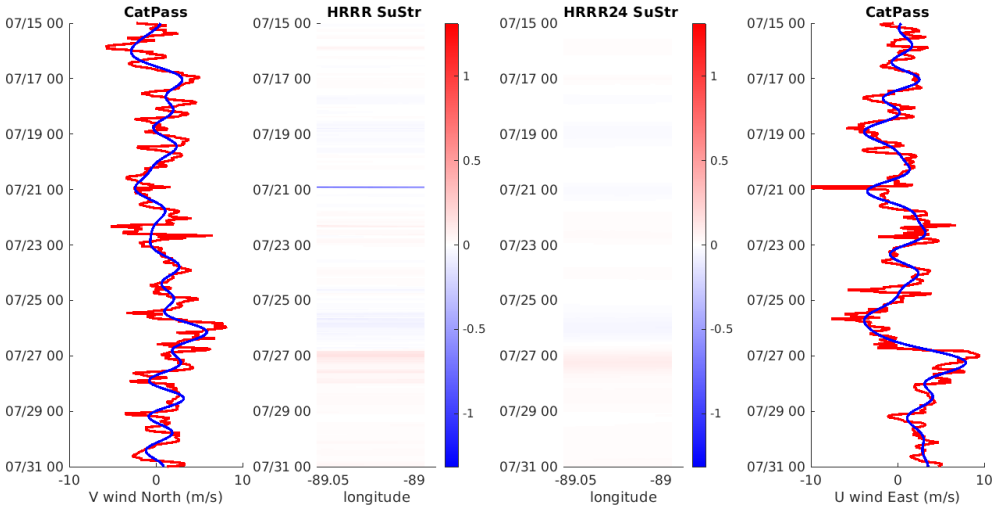

Cat pass Superficial stress comparison between u wind forcing HRRR vs HRRRR24

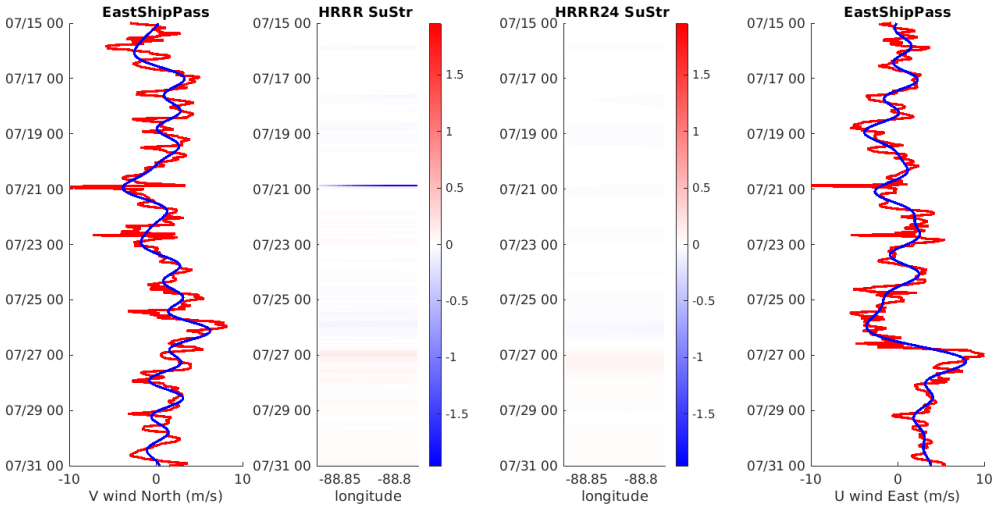

East Ship pass Superficial stress comparison between u wind forcing HRRR vs HRRRR24

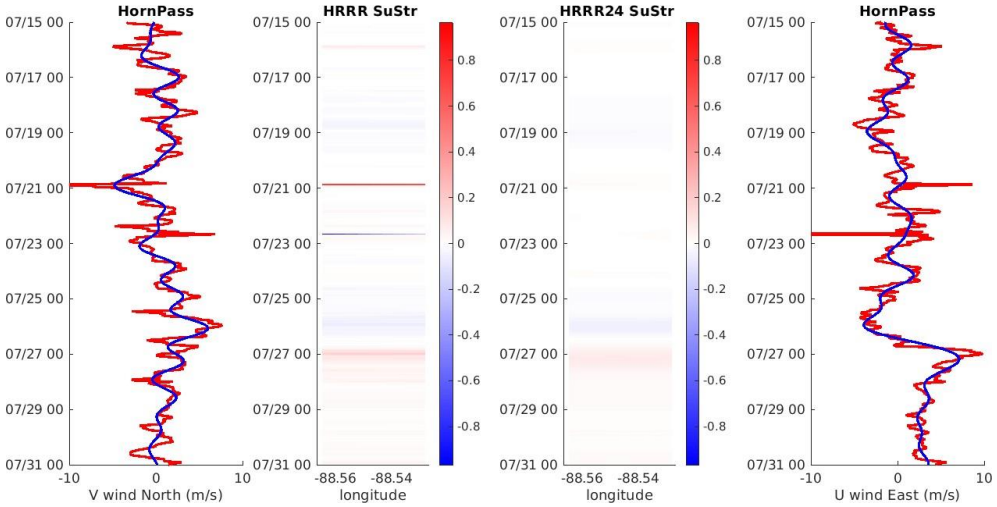

Horn pass Superficial stress comparison between u wind forcing HRRR vs HRRRR24

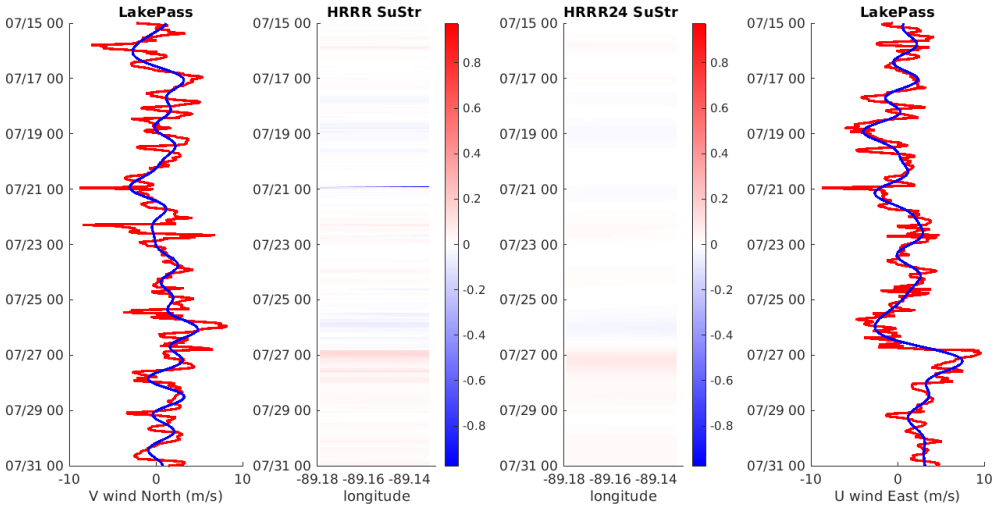

Lake pass Superficial stress comparison between u wind forcing HRRR vs HRRRR24

Superficial V vector stress:

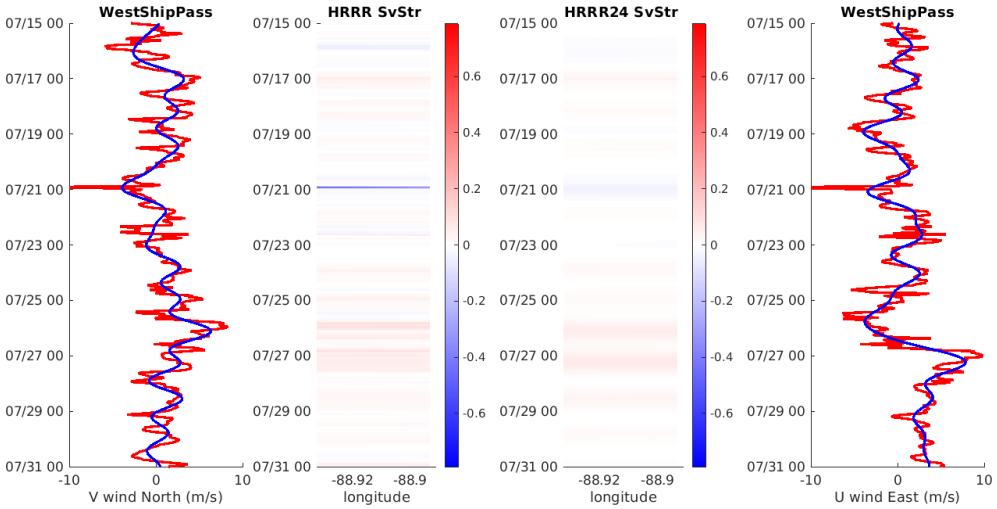

West Ship pass Superficial stress comparison between v wind forcing HRRR vs HRRRR24

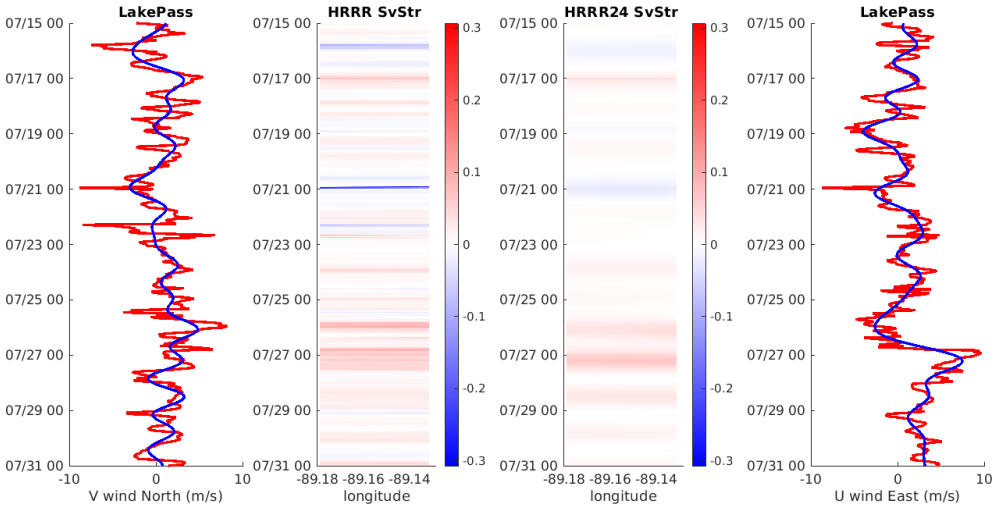

Lake pass Superficial stress comparison between v wind forcing HRRR vs HRRRR24

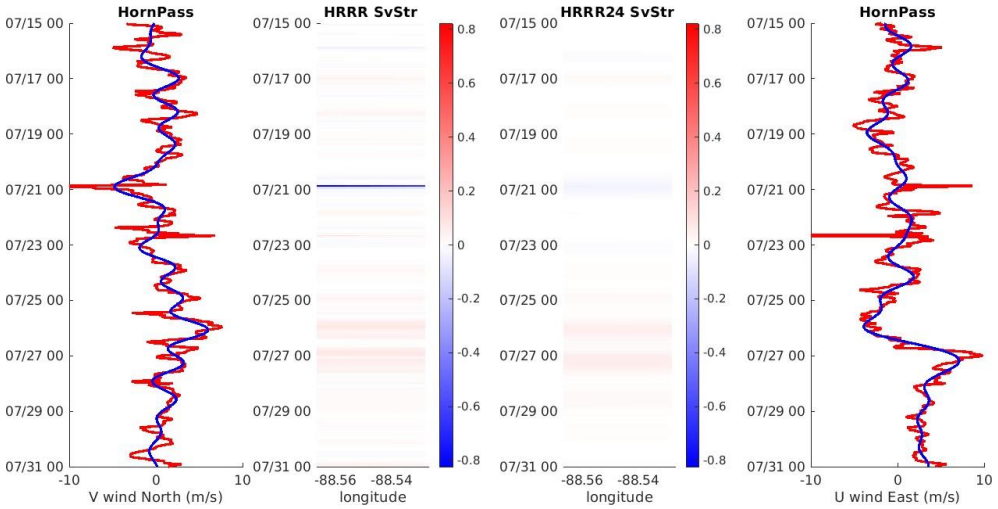

Horn pass Superficial stress comparison between v wind forcing HRRR vs HRRRR24

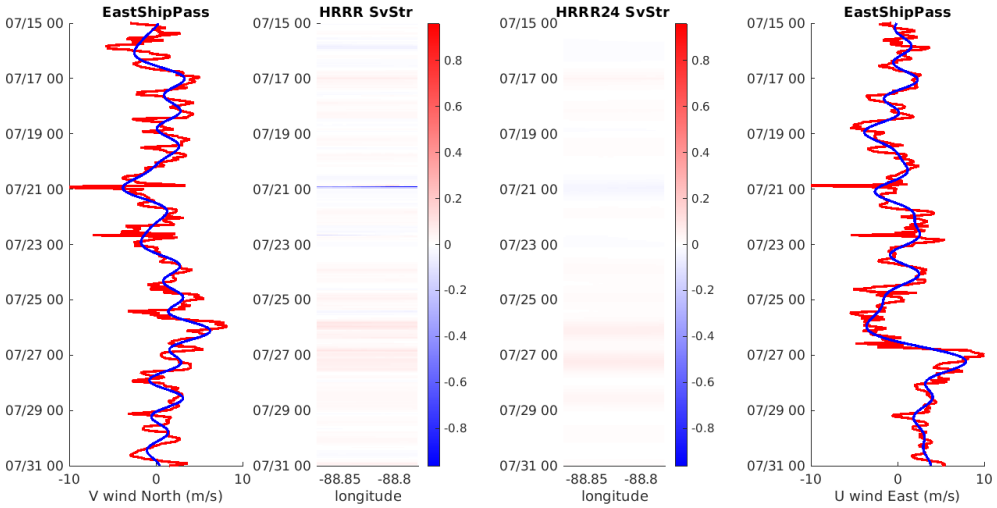

East Ship pass Superficial stress comparison between v wind forcing HRRR vs HRRRR24

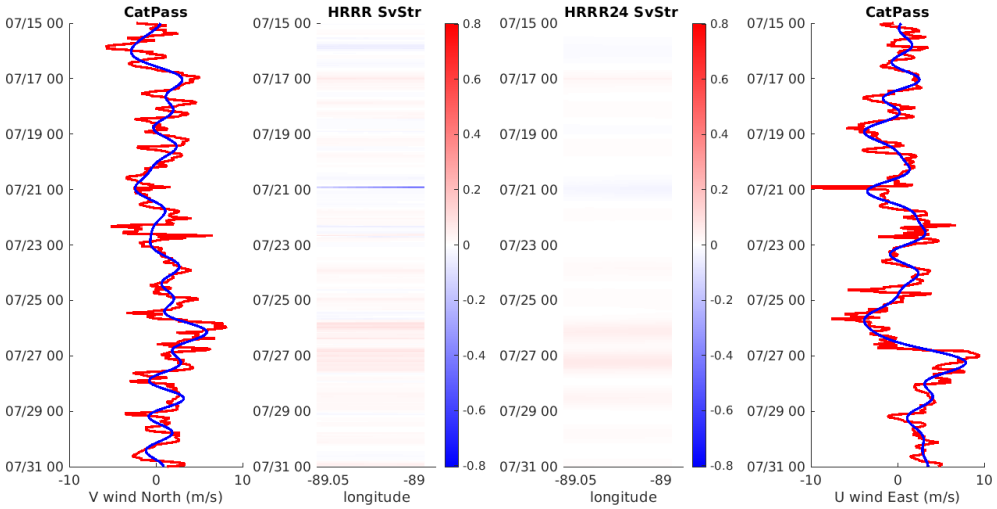

Cat pass Superficial stress comparison between v wind forcing HRRR vs HRRRR24